CONTROL OF HYDROGEN SULPHIDE EMISSIONS USING ZINC OXIDE NANOPARTICLES

A thesis submitted to the College

of Graduate Studies and Research

in partial fulfilment of the requirements

for the degree of Master in Environment and Sustainability

in the School of Environment and Sustainability

University of Saskatchewan

Saskatoon

By

Bennet Awume

PERMISSION TO USE

In presenting this thesis in partial fulfillment of the requirements for a Postgraduate degree from the University of Saskatchewan, I agree that the Libraries of this University may make it freely available for inspection. I further agree that permission for copying of this thesis in any manner, in whole or in part, for scholarly purposes may be granted by the professor or professors who supervised my thesis work or, in their absence, by the Head of the Department or the Dean of the College in which my thesis work was done. It is understood that any copying or publication or use of this thesis or parts thereof for financial gain shall not be allowed without my written permission. It is also understood that due recognition shall be given to me and to the University of Saskatchewan in any scholarly use which may be made of any material in my thesis.

Requests for permission to copy or to make other use of material in this thesis in whole or part should be addressed to:

Executive Director
School of Environment and Sustainability
University of Saskatchewan
Room 323, Kirk Hall
117 Science Place
Saskatoon, SK S7N 5C8
Canada

ABSTRACT

Emission of hazardous gases such as hydrogen sulphide (H_2S) by a variety of industrial processes and as a result of agricultural activities has become an issue of great concern over the years. The control of these gases is needed to ensure public safety, to protect the environment, and lastly to comply with occupational and environmental regulations. Several techniques including biological and physicochemical methods have been applied to remove these gases from contaminated air streams.

In this work, Zinc oxide (ZnO) nanoparticles were used to adsorb H_2S gas at ambient temperatures. The effects of H_2S concentration (80-1700 mg L^{-1}), nanoparticle size (18, 80-200 nm), gas flow rate (200 and 450 mL min^{-1}), temperature (1-41°C) and adsorbent quantity (0.2-1.5 g) were investigated in the laboratory scale. A semi-pilot system was also developed and used to treat H_2S emission from stored swine manure. The results show that when H_2S concentration was increased the adsorption capacities (both breakthrough and equilibrium) increased and the nanoparticles reached the saturation state faster. When nanoparticles of different sizes were tested, it was observed that 80-200 nm particles got saturated with H_2S faster than 18 nm particles. The adsorption capacities were higher with 18 nm particles than those with 80-200 nm. Temperatures did not have an effect on how fast the nanoparticles got saturated and on breakthrough adsorption capacity, but equilibrium adsorption capacity increased due to increase in temperature. The breakthrough and equilibrium adsorption capacities increased with increased quantity of nanoparticles. BET isotherm described the equilibrium data with higher accuracy as compared to other adsorption isotherms which were tested. Semi-pilot scale tests proved the effectiveness of 18 nm ZnO nanoparticles in capture of H_2S emitted from stored swine manure. For an experimental period of approximately 100 minutes the level of H_2S was reduced from an average initial value of 235.7±85.2 mg L^{-1} to a negligible level (an average value of 0.26 mg L^{-1}) corresponding to an H_2S removal of at least 99%. Semi pilot tests also showed that 18 nm ZnO nanoparticles were able to capture about 74% of NH_3 that passed through the adsorption column.

ACKNOWLEDGEMENTS

I first want to thank the Almighty God for the strength and wisdom he granted me throughout my academic and research program at the University of Saskatchewan.

I would like to express my sincere appreciation to my supervisors, Dr. Mehdi Nemati and Dr. Bernardo Predicala, for their guidance and encouragement throughout my research.

My sincere gratitude also goes to the members of my graduate student advisory committee, Dr. Charles Maule and Dr. Catherine Niu for their valuation comments and suggestions.

I sincerely thank Richard Blondin and Heli Eunike for the help in GC troubleshooting. I also appreciate the technical assistance from Mehdi Tajallipour, Lyman Moreno, Alvin Alvarado and the staff of the Prairie Swine Centre.

I thank my family and friends for their endless love, support and inspiration. I would never have gotten this far without them.

DEDICATIONS

I dedicate this thesis to my parents Mr. and Mrs. Awume who have always been there for me.

TABLE OF CONTENTS

LIST OF TABLES

LIST OF FIGURES

1. INTRODUCTION

Air pollution is one of the major causes of diseases in human and animals as well as environmental degradation. When the emission of hazardous gases and odour are not prevented from the sources or controlled, they are released into the environment and this leads to several undesirable effects. Most of these gases have characteristic pungent odours. Some of them are directly harmful when emitted into the atmosphere and others react with certain compounds to form harmful secondary particulates. In order to sustain the health of human, animals and the environment now and in the future, development of effective ways for controlling the emission of hazardous gases is essential.

Hazardous gases such as hydrogen sulphide (H_2S) and ammonia (NH_3) are usually produced as part of several industrial processes. In swine production, these gases are produced in the barns and manure storage structures during manure handling and storage processes. Emission of H_2S and NH_3 is a major concern because of the associated adverse effects they have on human, animals and the environment.

Hydrogen sulphide is produced as by-products of anaerobic decomposition of manure constituents such as sulphur-containing amino acids. It is formed when bacteria decompose sulphur-containing amino acids in animal excreta (Arogo et al., 2000). Exposure of humans and animals to this gas can cause several health problems such as unconsciousness, loss of productivity and even death (ASABE, 2005b). Hydrogen sulphide may be oxidized to sulphur dioxide (SO_2) which can lead to some undesirable adverse effects such as acidic deposition, smog and haze (ATSDR, 2006). Many human fatalities have been recorded as a result of livestock exposures to high level of H_2S (Curtis, 1983). Hydrogen sulphide concentrations as high as 1000 mg L^{-1} have been recorded in swine operations (Chenard et al, 2003), while concentration of 100 mg L^{-1} is considered dangerous to life and health of humans under the Respiratory Protection Guidelines of the Canadian Centre for Occupational Health and Safety (CCOHS, 2005). The continuous emission and associated adverse effects of H_2S and other odorous gases have led to major occupational health concerns and the development of strict environmental and occupational regulations. These regulations are gradually being enforced and non-compliance can have serious consequences, including forced discontinuation of operations.

To ensure safety of workers, animals and public, to protect the environment, and to comply with these strict rules, industries must find efficient techniques to reduce hazardous gas emissions.

Research has been carried out in the quest to address the problem of hazardous gas emissions in swine production. Some of the investigated gas emission techniques include diet manipulation, manure storage cover, manure additives, oil sprinkling and biofiltration. Manure storage covers are mainly used to reduce the emission of hazardous gases from manure storage sites and to biologically decompose gases that are emitted (Bussink and Oenema, 1998). This technique has proven to be good in reducing odour, but not effective in reducing hazardous gas levels (Koppolu et al., 2005). Diet manipulation involves the modification of animal feed to reduce the production of gas and odour (ASABE, 2007). This technique alone does not reduce the problems of hazardous gas emission since gas and odour are still produced (ASABE, 2007). Manure additives are more commonly used and are able to reduce gas and odours levels in the swine production facilities. Manure additives are used to directly adsorb NH_3 and H_2S, reduce the manure pH, inhibit microbial activity, or promote immobilization of microbes to reduce emissions of hazardous gases from manure (Arogo et al., 2001). The use of manure additives is expensive, especially when used in large scale facilities (Shah et al., 2007). Moreover, additives usually require repeated applications because their effectiveness lasts only for a brief period of time (McCrory and Hobbs, 2001). The oil sprinkling technique is used to mainly reduce dust and in some cases gas and odour emission in livestock facilities basically by sprinkling oil on the manure (Ouellette et. al, 2006). However, this technique is very costly and can lead to some safety problems in the facilities (Powers, 2004). Biofiltration is a biological process that uses microorganisms to purify polluted air before it is released into the atmosphere. The operating cost of biofilters can be very high because of high pressure drop occurring across the filter media (Riskowski, 2004).

Nanotechnology is a relatively new development that has aroused the interest of scientists and various industries for its varied potential applications. This technology involves the use of certain processes to develop microscopic materials with dimensions measured in nanometers, which have specific and unique chemical and physical properties (Morris et al., 2007). Advances in nanotechnology have led to development of nanoparticles with high surface area, high reactivity

and adsorption capacity (Ju-nam and Lead, 2008). Earlier studies have shown that nanoparticles are effective in water treatment and air purification (Khaleel et al., 1999; Hu et al., 2005). There is the need to explore this new and exciting technology in control of hazardous gases emission. Earlier work in application of nanoparticles for mitigation of hazardous gases emissions have focused mainly on gases at high temperatures and little information exist on this topic at ambient temperature. The objective of this thesis was to investigate the adsorption of H_2S on nanoparticles as a means to control the emission of this harmful gas.

2. LITERATURE REVIEW, KNOWLEDGE GAP AND OBJECTIVES

2.1. Background

Several industrial processes including livestock production emit hazardous gases such as hydrogen sulphide (H_2S) and ammonia (NH_3) during their operations. The main livestock operations associated with the emission of H_2S and NH_3 are swine, cattle and poultry (Atia, 2013). Canada has a large swine production industry, being ranked sixth in world swine production with about 13 million pigs as recorded in 2013 (Statistics Canada, 2014). Therefore emission of hazardous gases (i.e. H_2S and NH_3) from such industry poses risk to workers, animals and negatively impacts the environment.

Hydrogen sulphide is a major gas produced during swine production (Barrasa et al., 2010; Moreno et al., 2010). In swine production, this gas is produced in the barns and manure storage structures as well as during manure treatment and application. Hydrogen sulphide emission occurs as a result of manure production and handling (Park et al., 2005). Manure is a by-product of livestock production and it contains several nutrients such as nitrogen, phosphorus and potassium (Zhang, 2011). It is usually stored for long periods and then used as fertilizers. Hazardous gases are produced through anaerobic decomposition by microorganisms or by chemical reactions that occur in the manure (Predicala et al., 2008). When the production of manure increases, the amount of nutrients available to be metabolized by microorganisms also increases and this results in increased production of gases such as H_2S and NH_3 (Asis, 2008).

2.2. Hydrogen sulphide generation in swine production

Animal manure is composed of a mixture of animal urine and faeces and is considered as slurry based on its dry matter content (MWPS, 2004). Typical manure generated by pigs is made up of around 90% water and 10% solid on average. The characteristics of manure are dependent on factors such as animal diet composition, animal age and the stage of production (MWPS, 2004). In most production facilities, manure is temporarily stored in pits; this usually changes the characteristics of the manure because of some physical, chemical and biological processes including drying and volatilization that take place (ASABE, 2005a).

Hydrogen sulphide is generated in manure by assimilatory and dissimilatory sulphate reduction (Moreno et al., 2010). During dissimilatory sulphate reduction, H_2S is produced by reduction of sulphate by anaerobic sulphate reducing bacteria. Sulphate reducing bacteria are anaerobic microorganisms that utilize sulphate and other inorganic sulphur compounds as electron acceptor during the oxidation of organic and inorganic compounds for their growth; thereby producing sulphide (Blunden, 2006). Sulphate in manure originates from animal feed. During assimilatory reduction, H_2S is generated by anaerobic decomposition of proteins. The organic sulphur portion of decomposing manure decreases as proteins are broken down into amino acids. The amino acids are degraded further to form sulphide (Clanton and Schmidt, 2000). After the H_2S has been produced it usually stays at the surface and in the manure slurry unless the manure is agitated.

2.3. Characteristics of hydrogen sulphide

Hydrogen sulphide is highly toxic and corrosive (Haimour et al., 2005; Sayyadnejad et al., 2008; Tang et al., 2009; An et al., 2010). It is colorless and has a pungent smell like rotten eggs (Sayyadnejad et al., 2008) and it is slightly lighter than air (1.19 times higher at 20°C and 101.1 kPa). It usually accumulates in pits and unventilated parts of the swine production buildings. Generally, H_2S levels in swine production facilities are low but significantly higher levels are produced (200-1000 mg L^{-1}) whenever manure is agitated (ASABE, 2005b). The levels could be much higher if the buildings are not well ventilated (Heber er al., 1997). Patni and Clarke (2003) recorded up to 1300 mg L^{-1} of H_2S in a grow-finish room during manure agitation. Christianson et al. (2004) noted that significantly high levels of H_2S can be recorded in production facilities during manure pump out, emptying manure pits, usage and maintenance of manure handling equipment, and high-pressure washing.

Exposure limits of humans to H_2S have been established to protect workers in occupational environments. The threshold limit values (TLV) are expressed in the time-weighted average (TWA) and short-term exposure limit (STEL). Time-weighted average is the gas concentration which humans can be exposed to for 8 hours without experiencing negative health effects and short-term exposure limit is the gas concentration which humans can be continuously exposed to for 15 minutes without experiencing negative health effects. Recently, the TWA and STEL for

H_2S have been reduced to 1 and 5 mg L^{-1}, respectively (ACGIH, 2010); these values are typically adapted in regulations by various Canadian jurisdictions.

Also, H_2S concentration of 100 mg L^{-1} has been set as immediately dangerous to life and health (IDLH) for humans. This was established to ensure that people in situations with this level of exposure should immediately take appropriate measures to reduce or eliminate the exposure (CCOHS, 2005).

2.4. Effects of H_2S on human, animals, and environment

The emission of H_2S imposes serious adverse effects on human, animals, and the environment. Exposure to H_2S can cause unconsciousness and even death in workers and animals. When the gas enters the human body through inhalation, it dissolves in the bloodstream and is carried throughout the body. Hydrogen sulphide in the body affects the respiratory control centre in the brain which then affects breathing. This causes the oxygen in the blood to be used up and the heart to stop functioning (Bhamhani and Singh, 1991). Low concentrations (0.0005 to 0.3 mg L^{-1}) of H_2S are easily detected by human senses (ATSDR, 2006); however, the senses may not be able to detect the differences between low and high concentrations. Table 2.1 summarises the effects of H_2S on human health.

Table 2.1. Effects of H_2S on human (ASABE, 2005b)

H_2S Concentration (mg L^{-1})	Effects on human beings
0.005	Barely detectable
4	Easily detectable, moderate odour
10	Eye irritation
27	Unpleasant odour
100	Coughing, eye irritation, loss of smell after 2 – 15 min exposure
200 – 300	Eye inflammation and respiratory tract irritation after 1 hour
500 – 700	Loss of consciousness and possible death in 30 – 60 min
800 – 1000	Rapid unconsciousness, cessation of respiration and death
1000	Diaphragm paralysis on the first breath, rapid asphyxiation

When pigs are exposed to at least 20 mg L^{-1} of H_2S, they begin to fear light, lose appetite and become nervous. At 50 – 240 mg L^{-1} exposure levels, pigs begin to vomit. They also eventually have diarrhoea and nausea. At levels above 800 mg L^{-1}, the animals experience sudden nausea, unconsciousness and even death (ASABE, 2005b).

Hydrogen sulphide can stay in the atmosphere for about 18 hours. While in the atmosphere, it can transform to sulphur dioxide (SO_2) and eventually sulphuric acid (H_2SO_4) which is the major component of acidic deposition (ATSDR, 2006). Also, it contributes to the deterioration of production facilities and equipment due to its corrosive nature (Assaad et al., 2008).

2.5. Control of hazardous gas emission in swine production

There are several technologies that have been proven effective in reducing hazardous gas concentration in swine production. Some of these reduce the gas levels after it has been produced, while others stop or reduce the production of the gas. Some of these techniques are discussed in the following sections.

2.5.1. Diet manipulation

Diet manipulation involves the modification of animal feed to reduce the production of hazardous gas and odour (ASABE, 2007). Animal feed can be altered to make it more digestible or the feed composition can be changed. When the protein content of animal diet is modified to match the amount of amino acid the animals need, it reduces the excretion of excess nutrients and consequently the production of odour and hazardous gases such as H_2S and NH_3 (Sutton et al., 1999; ASABE, 2007). Diet manipulation technique can reduce the production of gases and odour from manure while not affecting the animal's productivity (McGinn et al., 2002).

According to a study conducted by Hobbs et al. (1996), when crude protein is reduced in animal diet from 21% to 14%, nitrogen excretion is reduced from 19% to 13%. Also, when crude protein and synthetic amino acids are reduced, nitrogen excretion is reduced by 40% (Sutton et al., 1999). Similarly, Kendall et al. (1998) showed that when crude protein is reduced by 4.5% and the diet is modified with synthetic amino acids, odour and NH_3 emissions are significantly reduced. A study by Le et al. (2009) indicated that when crude protein is decreased from 15% to 12%, and the same amount of amino acids is supplemented for animals, NH_3 emission is reduced by 9.5%. In addition, a study by Godbout et al. (2001) which focused on the effect of dietary manipulations using low protein diet and canola oil sprinkling proved that the use of low protein diets reduces ammonia emissions by 30%.

Diet manipulation is not used in many facilities because the application of this method alone does not solve the problem of gas emission since some amount of gas and odour will still be produced (ASABE, 2007). Also, there is the need to carry out more studies to prove results and to determine the cost of new diet modifications (Sutton, et al., 2001).

2.5.2. Manure storage covers

Manure storage covers are mainly used to limit the emission of hazardous gases from manure storage sites and in some instances to create biologically active sites on the covers to biologically decompose gases that are emitted (Bussink and Oenema, 1998). It is important to cover the

surface of manure because the velocity of air over stored manure surface affects the release and distribution of gases and odour from manure (Asis, 2008). Bussink and Oenema (1998) reported that the emission of hazardous gases from open manure storage sites were more than that in closed sites.

Clanton et al. 1999 carried out tests to evaluate the performance of straw mat, vegetable oil mat, straw/oil mat, clay ball mat, PVC/rubber membrane and geotextile membrane as manure covering material. Swine manure was used for the tests and odour and H_2S levels were tested. The results proved that all the covers tested reduced H_2S and odour levels by 46% and 37% respectively. PVC/rubber membrane cover however was noted as the most effective in reducing odour and H_2S levels.

According to a study conducted by Bicudo et al. (2004), the geotextile covers significantly reduced odour, H_2S and NH_3 emission rates in swine manure storage facilities. They, however, are difficult to manage and cause safety problems during manure agitation and pumping.

Koppolu et al. (2005) also carried out a study of the benefits of using fine ground rubber covers on manure storage units. Their results show that when 3 inches of fine ground rubber cover was used on manure storage tanks, odour emission was reduced by 77% - 99%. With 2 inches fine ground rubber cover was used on lagoons, odour emission was reduced by about 44%. Manure storage covers have proven to be effective in reducing odour, but not hazardous gas levels (Koppolu et al., 2005).

2.5.3. Manure additives

Manure additives are used to adsorb NH_3 and H_2S directly, reduce the manure pH, inhibit the microbial activity causing generation of odors and other gases, or to promote immobilization of microbes to reduce emissions of hazardous gases from manure (Arogo et al., 2001). In swine production, application of different additives has been evaluated as a direct approach to prevent and/or control emission of H_2S.

McCrory and Hobbs (2001) observed that hydrogen cyanide (HCN) significantly reduced H_2S and odorous compound emissions from pig slurry. Zeolite can also be used to reduce NH_3 emissions in swine production facilities when it is applied in pits (Portejoie et. al, 2003).

Smith et al. (2004) carried out a study to investigate the effectiveness of aluminum chloride ($AlCl_3$) as a pH modifier. It was noted that when 0.75% (v/v) of $AlCl_3$ solution was added to the manure, pH level dropped from 7.48 to 6.69 and ammonia level decreased by 52%.

In another study, an additive named Bio-Kat, was sprayed in 5 barn pits and a lagoon at varying concentrations. The results showed that NH_3 levels significantly decreased with increased concentration of Bio-Kat applied (Schneegurt et al., 2005).

According to Shah et al. (2007), oxidizing agents such as hydrogen peroxide and potassium permanganate not only oxidize odorous organic materials but they also destroy bacteria which enhance the production of H_2S and NH_3.

Predicala et al. (2008) investigated the use of Na-nitrite and Na-molybdate to control H_2S emission from swine manure. They reported that the addition of 80mM nitrate or 2mM molybdate separately or simultaneously decreased H_2S emission from 500 $\mu L\ L^{-1}$ to 2-25 $\mu L\ L^{-1}$. In a similar work, Moreno et al. (2010) also investigated the use of Na-nitrite and Na-molybdate to control H_2S emission from swine manure in large scale. Results from their work showed that both compounds were able to decrease H_2S emissions. Hydrogen sulphide emission was controlled by 0.1 – 0.25 mM molybdate. It was also noted that the amount of nitrate or molybdate needed to control the emissions decreased as manure age increased.

It is noted however, that some additives lead to other problems such as corrosion in the facilities (Shah et al., 2007). Also disinfectants cannot be used widely in large scale because they neutralize rapidly and require repeated application (McCrory and Hobbs, 2001). In most cases, it is expensive to apply this technology because large amounts of the additives are needed to be applied to manure.

2.5.4. Oil sprinkling

The oil sprinkling technique has been adopted in the past mainly to reduce dust levels inside animal production facilities (Powers, 2004). However, studies have shown that oil sprinkling also reduces gas emission. Gases and odorous compounds usually bond to dust particles; thus, oil sprinkling can reduce odour as well as the transport of gas compounds through the removal of dust (Ouellette et al., 2006).

Godbout et al. (2001) tested the effect of canola oil and diet manipulation on gas and odour emissions in swine buildings. Their results showed that when canola oil was used alone, it did not have any significant effect in reducing the emission of the gases (including H_2S and NH_3). However, when low protein diet was used, NH_3 emission was reduced by 38%. Heber et al. (2004) carried out experiments to investigate the effects of oil sprinkling on concentrations of NH_3, H_2S and other gases. They reported that soybean oil sprinkling was able to reduce the concentration of the gases, as well as dust levels. Kim et al. (2008) tested the effectiveness of soybean and essential oils (herb and ravenda) to reduce hazardous gas and odour emissions. The results from that study indicated that after 24 hours of application, essential oil was most effective in reducing gas and odour levels. Studies have proven that dust and hazardous gas concentrations can be reduced to about half of the initial concentration when sprayed with oil water mixture (Banhazi et al., 2010).

Oil sprinkling technique is very cost effective and easy to apply in animal production facilities. However, it imposes several safety problems in the facilities (Powers, 2004). The application of oil can cause the floor of the barns to be slippery and this can result in injury to the workers. Machines such as fans and heaters which are used in the animal production facilities are susceptible to damage by fine oil droplets, thus oil must be carefully applied so that it does not affect their function. The application of oil sprinkling will therefore require effective maintenance of machines and the animal production facilities (Schmidt and Heber, 2004).

2.5.5. Bioscrubbing

Bioscrubbers are used to remove hazardous gases from contaminated air streams. They absorb H_2S in contaminated streams in liquid before biologically oxidizing the absorbed H_2S to sulphur or sulphate (Syed et al., 2006).

Potivichayanon et al. (2006) carried out a study using a fixed novel bioscrubber to remove hydrogen sulphide. *Acinetobacter sp.* MUI-03 and *Alcaligenes faecalis* cultures were used in the bioscrubber system. The results showed that the system was able to remove 98% of H_2S. It was also observed that the removal efficiency increased when the gas flow rate was decreased.

Shah et al. (2008) tested the use of bioscrubbers with polypropylene screen running in alum solution to reduce gas emissions in swine barns. The results indicated that the bioscrubber reduced NH_3 emissions by 58.3% after 66 hours of monitoring and evaluation. The use of bioscrubbers has proven effective in minimizing hazardous gases and dust levels in barns. However, cost effectiveness of these systems, as well as issues concerning pressure drop and large scale application need to be investigated (Shah et al., 2008; Lemay, 1999).

2.5.6. Biofiltration

Biofiltration is a biological process that uses microorganisms to purify polluted air before it is released into the atmosphere. Contrary to bioscrubbers, absorption of contaminated compound in an aqueous solution is not required in biofilters. Biofilters use microorganisms to break down undesirable organic and inorganic components of air and produce CO_2, water and biomass. The biofilters are made up of porous solid media on which the microorganisms grow; the media also allows the effective flow of contaminants through the system. Target gases that flow through the filter are then oxidised by the microorganisms present in the biofilter (DeBruyn, 2000). The media used in biofilters are usually biological residue such as peat and compost (Nicolai and Janni, 2001).

This technology is effective in reducing the concentrations of hazardous gases in livestock buildings. Chung et al. (1999) used biofilters with *Thiobacillus thioparu* CH11 and *Nitrosomonas europaea* to treat mixture of H_2S and NH_3. The biofilter with co-immobilized cultures was fed with H_2S and NH_3 gases. Results from the experiment showed that the microorganisms were effective in reducing the level of the gases and the efficiency of the system remained above 95% regardless of amount of H_2S or NH_3 used.

DeBruyn (2000) carried out experiments in a 2000 head hog facility to test the reduction of odours in the barns during winter at reduced cost. It was reported that using experimental biofilters, H_2S and NH_3 concentrations were reduced by 56 – 100%. Also, between September and February (winter season), the efficiency of odour removal was between 69 – 87%.

Chang et al. (2004) investigated biofilter efficiency using a mixture of pine chaff and perlite as biofilter media. Results from the experiment showed that H_2S and odour levels were reduced by 82.4%. In a similar experiment, Chen et al. (2008) investigated the efficiency of biofilters in reducing odour using different types of filter medium (western cedar and hardwood wood chips). The results showed that both filter media were able to reduce odour and hazardous gas concentration significantly. On average, 51%, 41% and 83% reduction was recorded for odour, NH_3 and H_2S, respectively using western cedar wood chip biofilter.

Biofiltration has achieved some success in some areas but this technology has not been fully adopted in livestock operations because of its associated challenges. The effectiveness of a biofilter is dependent on good selection and management of the filter medium to provide appropriate conditions for the microbial population including temperature, concentration of gases, oxygen level, acidity, nutrients and moisture contents (Nicolai and Janni, 2001; Atia et al., 2013). The operating cost of biofilters can be very high; introduction of air at high pressure is required in order to allow its passage through the medium due to significant pressure drop occurring across the filter medium (Riskowski, 2004). Another downside of the application of biofilters in livestock facilities is the size of filters which are needed to treat large amount of gas/odour produced in barns and the short retention time involved (Lemay, 1999).

2.6. Nanotechnology

Nanotechnology can be described as the use of certain processes to manipulate matter on an atomic, molecular and macromolecular level to develop microscopic materials with dimensions measured in nanometers, which have specific and unique chemical and physical properties (Morris et al., 2007). This technology is not only about the size of materials but about the manipulation of the structure and ability of materials to function more effectively (Masciangioli and Zhang, 2003).

Nanomaterials can be grouped into 4 main types based on the materials that are used in making them. These are carbon-based materials which are made from carbon; dendrimers which are made from polymers; metal-based materials which are made from metals; and composites which are a combination of nanoparticles with other nanoparticles or larger materials (USEPA, 2007). For this work, the focus was on metal-based nanoparticales including metal oxides such as ZnO nanoparticles. Metal oxides are more stable under harsh processing conditions (Liu et al., 2009). Nanotechology can also be used to develop nanofilms, nanotubes and nanohorns (Masciangioli and Zhang, 2003). These are nanomaterials which vary in shape because of the order of their atoms and molecules.

The use of nanoparticles has aroused the interest of professionals in many fields because of their unique properties and characteristics. They have important characteristics that make them applicable in various industries and disciplines such as pharmaceuticals, electronics, environmental remediation, materials sciences and biomedicine (Lee et al., 2007; Wang et al., 2007; Ju-Nam and Lead, 2008; Tiede et al., 2009). They possess an advantage over traditional adsorbents depending on the characteristics of the adsorbent and adsorbate. This is because of their surface area, pore size distribution and surface chemistry (Shelly, 2003). Nanoparticles unlike other adsorbents have high percentage of their constituent atoms at the surface.

2.6.1. Properties of nanoparticles

The properties of nanomaterials differ significantly from that of the larger particles (Okuyama et al., 2006). Small pore size of the nanoparticles provides a large surface area which makes them very good adsorbents (Okuyama et al., 2006; Sayyadnejad et al., 2008). The large surface area creates more surface reaction sites with gas molecules and enhances effective interactions between the adsorbent and adsorbate (Khaleel et al., 1999; Ju-Nam and Lead, 2008). The amount of nanoparticles needed for reaction with other compound is minimized because of their large surface area which makes them highly efficient. Also, the small pore size creates more adsorption sites for adsorbate-adsorbent interraction.

2.6.2. Application of nanoparticles in environmental clean-up

The development of nanoparticles with unique properties has provided another alternative for cleaning and protecting the environment, as well as ensuring the health of human beings and livestock. Nanoparticles have been applied for various purposes including groundwater treatment, wastewater treatment, water and air purification. In most applications, nanoparticles have been either applied directly to the site or used in filters (Alvarado, 2011). Some studies described below have proven that nanoparticles can be used for environmental clean-ups (Khaleel et al.,1999; Cao et al., 2005; Hu et al., 2005).

This technology has been adapted in recent years for purification of air. Khaleel et al. (1999) tested the adsorption of some volatile organic compounds (propionaldehyde, benzaldehyde, ammonia, dimethylamine, N-nitrosodiethylamine and methanol) with nanocrystalline Magnesium oxide (MgO). The results showed that the MgO nanoparticles were able to adsorb the organic compounds and it is a better adsorbent than activated carbon. For every mole of organic compound, it was observed that 10 moles of MgO nanoparticles was able to quickly adsorb 50-80% of the compounds while similar amount of activated carbon adsorbed 10-40%.

Nanotechnology has also been applied in water purification and wastewater treatment processes. Hu et al. (2005) carried out a study using magnetic separation and meghamite nanoparticles

adsorption to remove and recover chromium (Cr (VI)) from wastewater. The results showed that the efficiency of adsorption was pH dependent, and the highest adsorption achieved at pH 2.5. In another research work, Cao et al., (2005) used iron nanoparticles and microscale iron powder to reduce the concentration of perchlorate-contaminated water. When iron nanoparticles were used in the reactors with 200 mg/L perchlorate concentration, 59.1% reduction was observed. Jain and Pradeep (2005) also studied the effectiveness of silver nanoparticles coated onto polyurethane (PU) foams in removing bacteria from water. The results showed that when water with bacterial concentration of 1×10^5 to 1×10^6 CFU/mL was passed through the filter, no bacteria was detected in the effluent.

2.6.3. Application of nanoparticles for H_2S removal

The use of nanoparticles in the control of H_2S emission and other air pollutants has been briefly explored in recent years. According to Wang et al. (2008), the effectiveness of a material in adsorbing H_2S depends on its characteristics. This makes it very important to carefully select the type of adsorbent for H_2S adsorption. Zinc oxide is an effective adsorbent for H_2S (Habibi et al., 2010) and has been widely used for the removal of H_2S and other gases. At ambient temperature, it is noted to have high equilibrium constant for H_2S adsorption (Wang et al., 2008). Zinc oxide is more stable and cost effective when compared with other adsorbents. The reaction between ZnO and H_2S produces zinc sulphide (ZnS) and water as shown in equation 2.1 below (Song et al., 2013):

$$ZnO_{(s)} + H_2S_{(g)} \rightarrow ZnS_{(s)} + H_2O_{(l)} \quad (2.1)$$

Some studies have used different nanoparticles to control H_2S emission under various conditions. Rosso et al. (2003) investigated the removal of H_2S by synthesized nanoparticles, using feed H_2S concentration of 100 mg L^{-1}, a flow rate of 400 mL min^{-1}, at 250 ˚C. The amount of adsorbent in a 2 cm long bench-scale reactor was 0.25 g. The breakthrough adsorption capacities reported for ZnO300 (surface area - 50.3 m^2/g) and ZnO400 (surface area - 43.3 m^2/g) were 0.03 and 0.02 g

H_2S adsorbed (g adsorbent)$^{-1}$, respectively. The equilibrium adsorption capacities for ZnO300 and ZnO400 adsorbents were 0.048 g H_2S adsorbed (g adsorbent)$^{-1}$.

Novochinskii et al. (2004) tested the removal of H_2S from steam-containing gas mixtures using ZnO sorbent (grains). A fixed-bed reactor connected to an H_2S analyzer was used for the tests. The adsorbent amount ranged from 0.92-4.00 g. The feed H_2S concentration and flow rate used were in the range 1-8 mg L^{-1} and 200-500 mL min^{-1}, respectively. The tests were performed at temperatures ranging from 300 to 400 ˚C. They reported a decrease in breakthrough adsorption capacity from 0.0041 to 0.0023 H_2S adsorbed (g adsorbent)$^{-1}$ as the particle size was increased from 0.053-0.075 to 3 mm, respectively. It was also indicated that the adsorption capacity was not affected when 0.053-0.075 mm particles were used. Also, a decrease in adsorption capacity from 0.0214 to 0.0049 was observed with increase in temperature from 300 to 400 ˚C.

Sayyadnejad et al., (2008) compared the effectiveness of ZnO nanoparticles and micron-sized ZnO in removal of H_2S from a drilling fluid. The tests were performed in a beaker where the adsorbents were mixed with drilling mud slurry. The results showed that under the same operating conditions, synthesised nanoparticles removed 800 mg H_2S L^{-1} completely in 15 minutes, while with micron-sized ZnO only 2.5% of H_2S was removed over a period of 90 minutes.

Wang et al., (2008) studied the effectiveness of SBA-15 supported zinc oxide (ZnO) nanoparticles in capturing H_2S. The SBA-15 supported zinc oxide (ZnO) nanoparticles were prepared by incipient wetness impregnation and ultrasonic method and in situ activation at 523 K. In their work, Wang et al. (2008) packed the adsorbent into a U-type glass adsorbent column, which was then attached to the entire set up. The system was operated with 0.1 % feed H_2S concentration and a flow rate of 500 mL min^{-1} at 298 K. It was reported that the system removed H_2S down to ppb irrespective of the amount of Zinc loaded. Also, the highest breakthrough adsorption of 0.436 H_2S adsorbed (g adsorbent)$^{-1}$ was observed when the column was packed with 3.04 wt% of zinc.

Asis (2008) evaluated the effectiveness of ZnO nanoparticles in reducing gas and odour levels using filtration and mixing methods in a semi-pilot scale setup. The results showed that filtration of a contaminated gas at a flow rate of 500 mL min^{-1} decreased H_2S concentration ranging from 23 – 42 mg L^{-1} by 74% to 99%. When the mixing method was used, H_2S concentration was reduced by 98%. In a similar work, Alvarado (2011) evaluated the use of ZnO nanoparticles to reduce H_2S, NH_3 and odour levels using filtration and mixing methods. The results showed that the mixing method achieved more than 98% H_2S reduction from initial concentration ranging from 500 – 750 mg L^{-1} but no major reduction of NH_3 was observed. The filtration method achieved some reduction in both H_2S and NH_3.

Habibi et al. (2010) investigated H_2S removal from natural gas stream using nano-zinc oxide (rodlike and spherical morphology) at feed flow rate of 1100 mL min^{-1}. The system setup comprised of a fixed bed reactor and a furnace. The feed gas concentration ranged between 5000-10000 mg H_2S L^{-1}. The breakthrough adsorption capacity reported for rod-like ZnO nanoparticle at 150 and 250 ˚C were 0.20 and 0.24 g H_2S adsorbed (g adsorbent)$^{-1}$, respectively. This showed a decrease in the breakthrough adsorption capacity as temperature was decreased from 250 to 150 ˚C.

Nassar and Pereira-Almao (2010) investigated the capture of H_2S using different metal oxide particles in an oilsand-packed bed column. The tests were performed using 200 mg H_2S L^{-1} and gas flow rate of 110 mL min^{-1} at 200 ˚C. They reported an increase in the slope of the breakthrough curves as temperature was increased from 25 to 200 ˚C. The authors noted that this observation meant an increase in the adsorption efficiency of ZnO with increase in temperature. They also tested the effectiveness of different metal oxides (ZnO, Al_2O_3, NiO and CuO) on H_2S adsorption and reported breakthrough adsorption capacity of 0.0004 g H_2S adsorbed (g adsorbent)$^{-1}$ when tested with ZnO particles.

Table 2.2 compiles the important information of all the works which have been discussed in the preceding sections. Data in this table include the adsorbent type, adsorbent size, temperature, H_2S concentration, gas flow rate, and breakthrough and equilibrium adsorption capacities. Tests with activated carbon by Xiao et al. (2008) were also included to be compared with ZnO

nanoparticles and ZnO microns. From the data presented in the table it is evident the ZnO nanoparticles are superior in the capture for H_2S than the micronic ZnO and activated carbon. Also, a close look at the data presented in this table also shows that the majority of the earlier works have been carried out at high temperatures and little information regarding this process at ambient temperatures which are experienced in swine production facility is available.

Table 2.2. Summary of the recent data published on adsorption of H_2S by different adsorbents

Reference	Adsorbent Type	Adsorbent size (nm)	Temperature (°C)	H_2S Concentration (mg L^{-1})	Flow rate (mL min^{-1})	Breakthrough adsorption capacity (mg H_2S g $adsorbent^{-1}$)	Equilibrium adsorption capacity (mg H_2S g $adsorbent^{-1}$)
Xiao et al. (2008)	Sodium carbonate - impregnated activated carbon	$(4\text{-}5)\times10^5$	30	200-1000	120		2.1-3.0
	Untreated activated carbon	$(4\text{-}5)\times10^5$	30	200-1000	120		7.7-9.3
Rosso et al. (2003)	ZnO300 (combustion synthesis; calcination at 300 °C)	$(2.5\text{-}4.5)\times10^5$	250	100	400	33	51
	ZnO400 (combustion synthesis; calcination at 400 °C)	$(2.5\text{-}4.5)\times10^5$	250	100	400	26	51
	ZnO500 (combustion synthesis; calcination at 500 °C)	$(2.5\text{-}4.5)\times10^5$	250	100	400	1	12.7
	ZnO600 (combustion synthesis; calcination at 600 °C)	$(2.5\text{-}4.5)\times10^5$	250	100	400	0.6	7.4
	ZnOu500 (urea method; calcination at 500 °C)	$(2.5\text{-}4.5)\times10^5$	250	100	400	0.2	1.8
	ZnOu700 (urea method; calcination at 700 °C)	$(2.5\text{-}4.5)\times10^5$	250	100	400	2	2.6
	ZnO (commercial)	-	250	100	400	5.3	13.2

Table 4.2 continued

Reference	Adsorbent Type	Adsorbent size (nm)	Temperature (°C)	H_2S Concentration (mg L^{-1})	Flow rate (mL min^{-1})	Breakthrough adsorption capacity (mg H_2S g $adsorbent^{-1}$)	Equilibrium adsorption capacity (mg H_2S g $adsorbent^{-1}$)
Novochinskii et al. (2004)	ZnO sorbent (extrudate)	3×10^6	300	8	200 - 500	4.4	-
	ZnO sorbent (grains)	$(1.5\text{-}2.5)\times10^5$	300	8	200 - 500	28.7	-
	ZnO sorbent (grains)	$(1.1\text{-}1.5)\times10^5$	300	8	200 - 500	29.9	-
	ZnO sorbent (grains)	$(0.5\text{-}0.75)\times10^5$	300	8	200 - 500	22.7	-
	ZnO sorbent (grains)	$(1.1\text{-}1.5)\times10^5$	350	8	200 - 500	15.5	-
	ZnO sorbent (grains)	$(1.1\text{-}1.5)\times10^5$	375	8	200 - 500	10.8	-
	ZnO sorbent (grains)	$(1.1\text{-}1.5)\times10^5$	400	8	200 - 500	5.2	-
Wang et al. (2008)	Mesoporous silica SBA-15 supported ZnO nanoparticles (0.5% Zn)	-	25	1000	500	36	-
	Mesoporous silica SBA-15 supported ZnO nanoparticles (1.2% Zn)	-	25	1000	500	95	-
	Mesoporous silica SBA-15 supported ZnO nanoparticles (3.1% Zn)	-	25	1000	500	436	-
	Mesoporous silica SBA-15 supported ZnO nanoparticles (4.4% Zn)	-	25	1000	500	49.9	-
	Mesoporous silica SBA-15 supported ZnO nanoparticles (9.0% Zn)	-	25	1000	500	38.9	-

Table 4.2 continued

Reference	Adsorbent Type	Adsorbent size (nm)	Temperature (°C)	H_2S Concentration (mg L^{-1})	Flow rate (mL min^{-1})	Breakthrough adsorption capacity (mg H_2S g $adsorbent^{-1}$)	Equilibrium adsorption capacity (mg H_2S g $adsorbent^{-1}$)
Song et al. (2013)	ZnO nanoparticles	-	Ambient	255	284	9.4	-
	Carbon nanotube supported ZnO nanoparticles (prepared by reflux reduction)	-	Ambient	255	284	17.4	-
	Carbon nanotube supported ZnO nanoparticles (prepared by microwave assisted reduction)	-	Ambient	255	284	31.7	-
	Graphite oxide supported ZnO nanoparticles (prepared by reflux reduction)	-	Ambient	255	284	50.1	-
	Graphite oxide supported ZnO nanoparticles (microwave assisted reduction)	-	Ambient	255	284	120.5	-
Habibi et al. (2010)	ZnO nanoparticles	56	150 - 250	5000 - 10000	1100	30-240	-

2.7. Adsorption theory

Adsorption refers to the transfer of liquid or gas molecules to a solid surface, where they form chemical bonds with the surface or are held on the surface of the solid through intermolecular forces (Seader and Henley, 1998). The difference in the energy levels causes the affinity between the molecules (Flood, 1967). The molecules adsorbed on the surface of the solid are referred to as adsorbate and the solid on which they are adsorbed is known as adsorbent. The surface where the solid and gas come in contact is known as the site of adsorption (Seader and Henley, 1998). In this work, the nanomaterials are the adsorbent and the H_2S gas is the adsorbate.

When gas molecules are adsorbed to the surface of a solid, there is either a weak interaction or a strong interaction between the solid or gas; these are known as physical and chemical adsorption, respectively (Seader and Henley, 1998). Physical adsorption occurs when the gas molecules are attached to the surface of the solid by van der Waals forces. During physical adsorption, there is heat loss; this is described as the heat of adsorption. As a result, the quantity of gas molecules adsorbed increases with the decrease in adsorption temperature. Multiple layers of the gas molecules could form on the solid surface as their quantity increases (Hines and Robert, 1985). In some cases, physical adsorption occurs with some amount of chemical activity; this is known as chemisorption. Chemical adsorption occurs when the interaction between the solid and gas molecules results in a covalent and/or ionic bond. When this happens, the structures of the gas and solid molecules as well as properties are changed. The presence of multiple layers in chemical adsorption is rare because of the strong bonds that are formed between the transferred gas molecules and the solid surface. In some instances, an increase in the quantity of gas molecules adsorbed increases with increase in temperature (Hines and Robert, 1985).

2.7.1. Adsorption capacity

Adsorption rate is defined as how quick or slow the adsorbate is taken up by the adsorbent. It is affected by the properties of the adsorbate and adsorbent, as well as the operating conditions such as flow rate, temperature etc. Breakthrough curves are used to describe how long the adsorbent takes to get saturated. It also shows the variation in adsorbate uptake with time. Figure 2.1 shows a schematic diagram of a typical breakthrough curve.

Adsorption capacity refers to the maximum amount of adsorbate that can be adsorbed per unit mass of the adsorbent. Equilibrium capacity also known as saturation capacity is the capacity of the adsorbent under equilibrium conditions. The equilibrium established at a given temperature and pressure for a given amount of gas depends on the properties of both the adsorbate and adsorbent. The adsorbent properties include the pore size distribution, size, shape and chemical composition. The breakthrough capacity refers to the capacity of the adsorbent at the breakthrough time. Breakthrough time is defined as when $\frac{C}{Co} = 0.05$ (Guo et al., 2007).

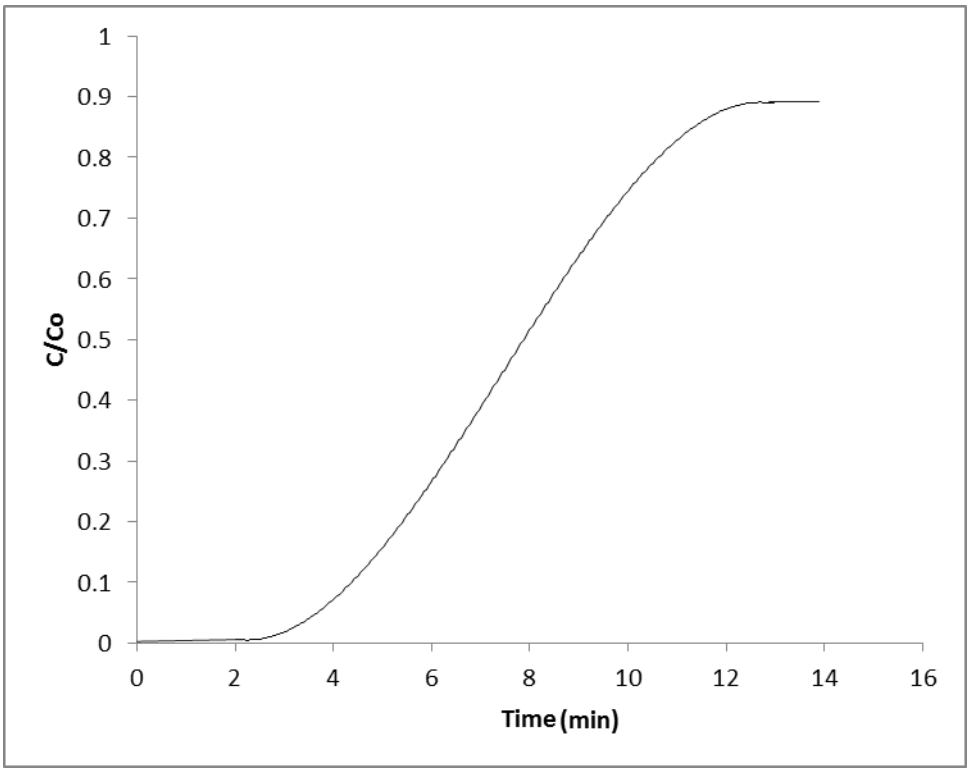

Figure 2.1. Schematic diagram of a breakthrough curve, where C is the effluent gas concentration and Co is the influent gas concentration.

2.7.2. Mass transfer (diffusional) limitations

There are two main resistances to mass transfer during the adsorption; micropore and macropore diffusional resistances. Micropore diffusional resistance is any barrier to the transfer of mass that occurs through the individual molecules of the adsorbent and the macropore diffusional resistance is any barrier to the transfer of mass that occurs within the bulk crystalline structure of

the adsorbate. The macropore resistance can be reduced by reducing the gross particle size of the adsorbent. The micropore resistance is, however, independent of the gross particle size (Ruthven, 1984).

2.7.3. Adsorption isotherms

Adsorption isotherms describe the relationship between gas and solid phase concentrations of an adsorbate at constant temperature (Hines and Robert, 1985). They can be obtained by calculating the adsorbed amount of adsorbate using the overall mass balance. The adsorption system must first reach equilibrium; that is, the state in which the temperature of the bed has been restored to its initial state and there is no mass transfer.

Generally, there are at least five main types of equilibrium isotherms. Type I, also known as Langmuir type is characterized as a monolayer adsorption. It is usually applicable in cases of chemical adsorption systems. Microporous adsorbents such as charcoal and silica gel exhibit this isotherm type. Type II is a multilayer adsorption and is exhibited by nonporous solids. It is also known as the Brunauer-Emmett-Teller (BET) isotherm. Type III isotherm also occurs as a result of the formation of multilayers. It is usually found when an island or drop nucleation is necessary for adsorption. Type IV occurs when there is pore filling as well as adsorption on the outer surface. Type V adsorption is found when there is pore filling and nucleation as well as outer surface adsorption. Type VI adsorption occurs when there in combination of two or more of the above types. They represent stepwise multilayer adsorption (Hines and Robert, 1985; Sing et al., 1985; Ranke, 2008).

Adsorption isotherm models include linear, Langmuir, Freundlich, BET, Langmuir-Freundlich, which are described by equations 2.2, 2.3, 2.4, 2.5, 2.6 below, respectively:

$$q = bc \tag{2.2}$$

$$q = \frac{q_s\, b\, C}{b+C} \tag{2.3}$$

$$q = bC^{1/n} \quad n > 1.0 \tag{2.4}$$

$$q = \frac{q_s\, bC^{1/n}}{1+bC^{1/n}} \tag{2.5}$$

$$q = \frac{q_s b\left(\frac{p}{p_s}\right)}{\left(1-\frac{p}{p_s}\right)\left(1-\frac{p}{p_s}+b\frac{p}{p_s}\right)} \tag{2.6}$$

where, C is the concentration of adsorbate in the gas phase (mg L^{-1}), q represents the adsorption capacity of the adsorbent (g H_2S adsorbed (g adsorbent)$^{-1}$), q_s is the saturation limit (g H_2S adsorbed (g adsorbent)$^{-1}$), p denotes sorbent partial pressure (kPa), p_S is the saturation vapor pressure (kPa), and b and n are the isotherm coefficients.

2.8. Knowledge gaps and objectives

Hazardous gas treatment techniques including diet manipulation, oil sprinkling and biofiltration have been applied to mitigate hazardous gas emission during swine production. However, there is still the need to find more efficient and cost-effective approaches to solve the problem. In recent years, nanotechnology has been applied for capturing of hazardous gases (i.e. H_2S) and has shown promising results. However, the application of nanomaterials to treat H_2S has not been extensively researched and there is still the lack of information on the optimum conditions (such as temperature, nanoparticles size, nanoparticle amount and feed flow rate) required for effective removal of H_2S. Furthermore, the majority of earlier research on application of nanoparticles has focused on control of gas emissions at temperatures which are way higher than those experienced in swine production (i.e. ambient temperature range). Therefore, in this thesis, the adsorption of H_2S by nanoparticles was investigated at ambient temperatures, with the aim of identifying the effects of various variables, determining the optimum conditions and to assess the effectiveness of this approach in a semi-pilot scale system.

2.8.1. Objectives

The main goal of this project was to investigate a treatment technology whereby nanomaterials are used to remove hazardous gases (i.e. H_2S) from the contaminated air streams (especially those emitted from swine production facilities). The specific objectives of this research were:

1. To determine the effects of H_2S concentrations (80-1700 mg L^{-1}), gas flow rate (200 and 450 mL min^{-1}), size of the nanoparticle (18, 80-200 nm), temperature (1-41°C) and quantity of the adsorbent (0.2-1.5 g) on the removal of H_2S.
2. To use a semi-pilot scale system to evaluate the effectiveness of the developed approach in treatment of gases emitted from stored swine manure.

3. MATERIALS AND METHODS

3.1. Nanoparticles

Two different size ranges of ZnO nanoparticles were obtained from US Research Nanomaterials, Inc. (Houston, TX) for this work. One had a particle size of 18 nm and specific surface area (i.e. total surface area per unit mass of the nanoparticles) in the range 40-70 m^2/g. The second one had a crystalline size range of 80-200 nm and specific surface area in the range 4.8-6.8 m^2/g. The commercial nanoparticles were tested for surface area, pore size and pore volume using a BET analyser (ASAP 2020, Micromeritics, USA). The results of these analyses are presented in Appendix C. As recommended by the manufacturers, a nose mask and rubber gloves were used while handling the nanoparticles.

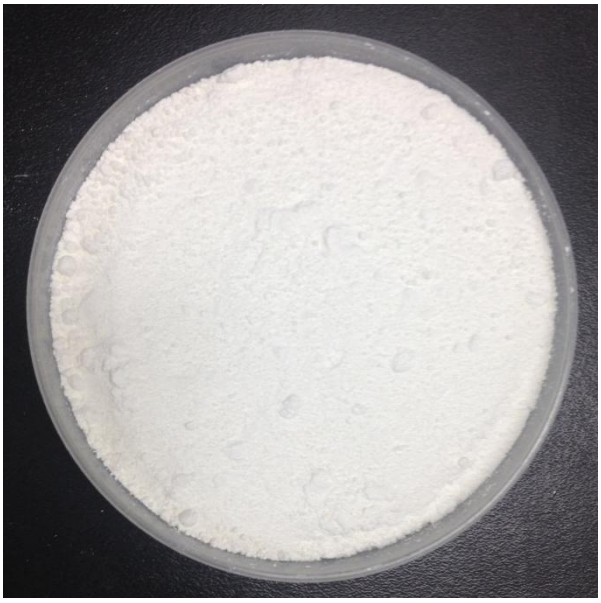

Figure 3.1. Zinc nanoparticles with 18 nm particle size.

3.2. Premixed gases and swine manure

Laboratory scale tests were conducted using industrial grade nitrogen gas (N_2) and premixed 1954 mg L^{-1} H_2S gas (balanced with N_2), both obtained from Praxair Canada Inc. (SK, Canada). These gases were used to test the adsorption of H_2S on nanoparticles and the effects of operating conditions on adsorption. After the laboratory tests, semi-pilot scale tests were conducted at the Prairie Swine Centre Inc. (SK, Canada) to test the effectiveness of the adsorption system in an actual livestock production facility. This was necessary because the composition of gas emitted

from the manure is different from the gases that were used in the laboratory tests. The main constituent of the gases emitted from manure is air, as opposed to N_2 which was the bulk gas in the laboratory tests. In addition to H_2S, the manure gas contains NH_3, other gases and moisture.

Semi-pilot scale tests were conducted using manure stored in containers to simulate the actual conditions in the swine barn. The manure slurry samples were collected from the underfloor manure pit of a grow-finish room at the swine barn at the Prairie Swine Centre Inc. (SK, Canada). Grow-finish rooms house the pigs at the grow-finish production stage (a period of about 14-16 weeks of raising nursery pigs until they reach to the market weight of 115-120 kg). Prior to collection of the manure samples, the manure in the pit was mixed thoroughly using a mechanical agitator to minimize manure variation in the collected samples. After which 12 clean 65-L containers were filled with 30 L of manure slurry. The fresh manure was covered in the containers and stored for 3 weeks at 20 °C to allow sufficient time for anaerobic digestion and production of manure gases.

3.3. Laboratory scale tests

3.3.1. Experimental set-up

The apparatus used for the laboratory set-up included the following: a glass adsorption column, mass flow meters (Aalborg, US), tygon tubing, sampling ports, differential pressure transducer (Honeywell, US), circulating water bath (VWR International, Canada), thermocouple (Omega K type, Stamford, USA) and a glass bottle containing scrubber solution (1 M NaOH solution). The schematic diagram and photograph of the experimental setup is shown in Figure 3.2.

A cylindrical glass tube which was supported by a clamp was used as the adsorption column. It had an internal diameter and length of 10 mm and 15 cm, respectively. A thin layer of glass wool was placed at the bottom of the column to maintain the powdery nanoparticles in the column. Then, the nanoparticles were loaded followed by another thin layer of glass wool and paper filter on top to prevent nanoparticles from blowing out from the top of the column due to the flow of gas. There was enough space between the top of the column and the loaded nanoparticles to keep

the bed fluidized during the tests. The fluidized bed was formed when the nanoparticles moved within the column freely like a fluid as the gas flowed through it.

The flow of the gas in the adsorption system was controlled using control valves and mass flow controllers. Clamps were used to block the flow of gas when it was necessary. Tygon tubing was used to connect the various components of the system because tygon does not react with H_2S. A differential pressure transducer connected to the top and bottom of the adsorption column was used to monitor the pressure change across the adsorption column during the tests. A water bath was used to circulate water through a devised jacket (spiral tygon tubing wrapped around the column) to maintain the adsorption bed temperature at the designated level. A thermocouple was inserted in the adsorption column to record the adsorption bed temperature. Gas samples were taken manually using air tight syringes through the sampling ports at different time intervals. The samples were analyzed for H_2S content using a gas chromatograph (GC) (Varian CP3800). A scrubber solution (1 M NaOH) was used to remove the residual H_2S in the outlet stream.

Nitrogen gas was used to test the system for leakages prior to each experiment. For safety purposes, the experimental set-up was placed inside a fume hood and a personal H_2S alarm was used by researchers while carrying out the experiments.

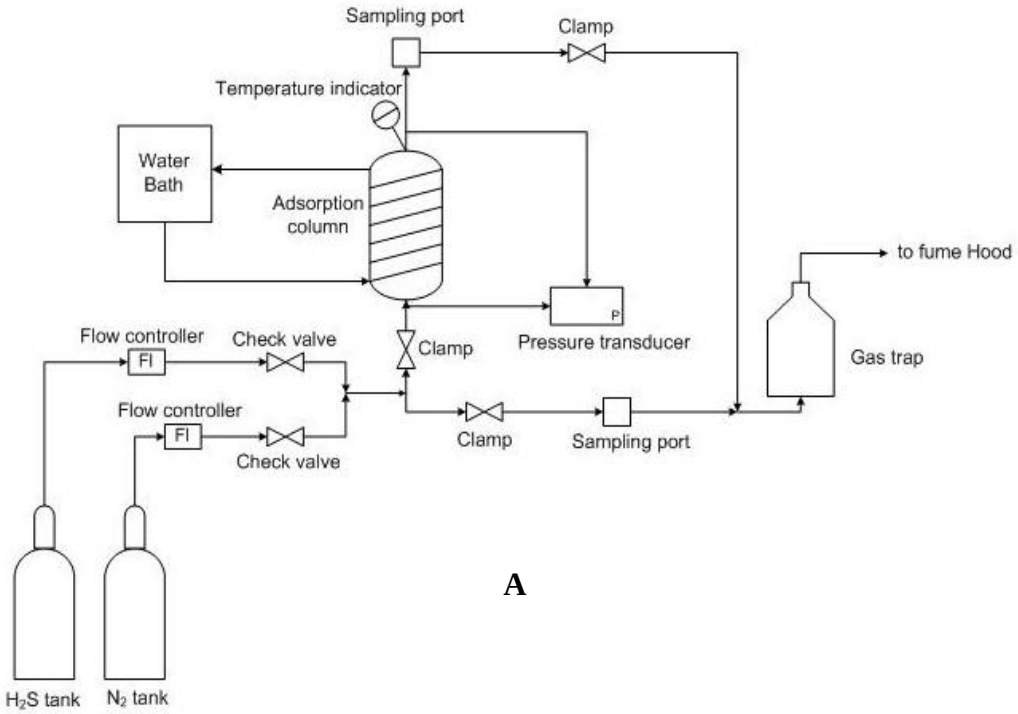

A

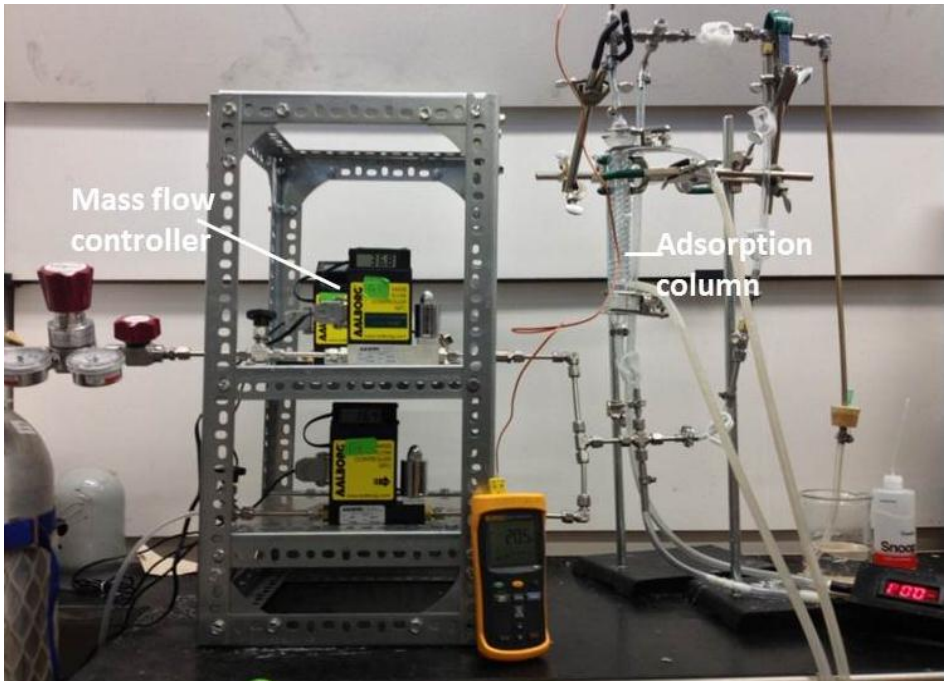

B

Figure 3.2. Schematic diagram (A) and photograph (B) of the laboratory scale set up

3.3.2. Experimental procedures

A series of laboratory scale experiments were conducted to investigate the adsorption of H_2S gas on nanoparticles. The system was used to treat gas streams contaminated with H_2S at different concentrations. Effect of gas flow rates, temperatures, nanoparticles sizes and nanoparticle bed depths were investigated.

Effects of H_2S concentration

Experiments to test the effects of H_2S concentration were conducted by varying H_2S concentration within the range of 80 to 1700 mg L^{-1}. Mass flow controllers were used to mix 1954 mg L^{-1} H_2S gas and N_2 to obtain the required feed concentration. A by-pass line devised for sampling of the gas prior to its introduction to the adsorption column was used for sampling and measurement of H_2S concentration in the diluted feed gas. The experiments were conducted at room temperature of 22±1 ˚C at a constant feed gas flow rate of 200±0.2 mL min^{-1}. The adsorption column was charged with 1 g of fresh ZnO nanoparticles (18 nm and 80-200 nm) in each experimental run. Gas samples were collected at regular intervals using a 1 ml gas tight syringe and were immediately analysed with a GC.

Effects of nanoparticle size

The effect of particle size was investigated using 18 nm and 80-200 nm ZnO nanoparticles. These sizes were chosen based on the availability of the nanoparticles from the supplier. The nanoparticles were used to test 5 different concentrations of H_2S ranging from 80 to 1700 mg L^{-1}. The experiments were conducted at room temperature of 22±1 ˚C using feed gas flow rate of 200±0.2 mL min^{-1}. The adsorption column was charged with 1 g of fresh 18 nm or 80-200 nm ZnO nanoparticles in each experimental run. Gas samples were collected at regular intervals using a 1 ml gas tight syringe and were immediately analysed with a GC.

Effects of gas flow rate

An additional experimental run with feed flow rate set at 450±0.3 mL min^{-1} was conducted to test the effect of gas flow rate on H_2S adsorption on nanoparticles. The test was conducted with feed concentration of 205 mg L^{-1} at 22±1 ˚C, using 1 g of fresh 18 nm ZnO nanoparticles. Gas samples were collected at regular intervals using a 1 ml gas tight syringe and were immediately analysed with a GC. The result was compared with the earlier experiment conducted with feed flow rate of 200±0.2 mL min^{-1} at the same temperature, nanoparticles quantity, nanoparticles size and gas concentration.

Effects of temperature

Experiments were carried out with adsorption bed temperatures at 1, 11, 22 and 41 ˚C to investigate the effect of temperature on H_2S adsorption. Feed H_2S gas concentrations ranging from 90 to 1600 mg L^{-1} were used. The adsorption column was charged with 1 g of fresh ZnO nanoparticles (18 nm) in each experimental run. The gas flow rate was kept constant at 200±0.2 mL min^{-1}. Gas samples were collected at regular intervals using a 1 ml gas tight syringe and were immediately analysed with a GC.

Effects of adsorbent quantity

To investigate the effect of adsorbent quantity, two sets of experiments were done. The first was conducted using average feed H_2S concentration of 1666.8 mg L^{-1} to test H_2S adsorption on 0.5, 1 and 1.5 g of fresh 18 nm ZnO nanoparticles. The second test was conducted using average H_2S concentration of 102.3 mg L^{-1} to test H_2S adsorption on 0.2, 0.5 and 1 g of fresh 18 nm ZnO nanoparticles. These experiments were carried out at 22±1 ˚C using gas flow rate of 200±0.2 mL min^{-1}. Gas samples were collected at regular intervals using a 1 ml gas tight syringe and were immediately analysed with a GC.

3.3.3. Adsorption kinetics and isotherms

Breakthrough curves were generated to study the effects of the various conditions on H_2S adsorption on ZnO nanoparticles. Breakthrough curves were used because they are suitable to assess the mass transfer resistances (Seader and Henley, 1998), as well as the period it takes for the adsorbent to get saturated. The breakthrough curves were generated by plotting C/C_0 versus time, where C represents the effluent H_2S concentration (mg L^{-1}) and C_0 represents the influent H_2S concentration in the feed stream. The breakthrough point was defined as the point where the ratio of the H_2S level in the effluent and that of the influent was ~0.05 (Guo et al., 2007). The breakthrough adsorption capacity was calculated using the experimental data from the start of the experiment to the breakthrough time. The system reached equilibrium state when the breakthrough curve levelled off and effluent H_2S concentration stabilized. At this point the bed was said to have reached saturation point. The equilibrium adsorptive capacity was calculated using the experimental data from the initiation of the experiment to the equilibrium point.

Equilibrium isotherms were developed at temperatures of 10 and 22 $^{\circ}$C for 18 nm ZnO nanoparticles and 22 $^{\circ}$C for 80 – 200 nm nanoparticles. This was done by plotting the adsorption capacity of the bed versus H_2S concentration in the gas phase. The equilibrium data were also fitted into different isotherm models to identify the most suitable expression. Langmuir, Freundlich, Langmuir-Freundlich, and BET adsorption models were tested.

3.4. Semi-pilot scale tests

3.4.1. Experimental set-up

The semi-pilot experimental set-up was a scale up of the laboratory scale system. It consisted of the following: a PVC adsorption column, centrifugal fan (Model Keho, Edwards group, Lethbridge, AB), thermal anemometer (VelociCalc 9545-A, TSI Inc., Shoreview, MN, USA), commercially-available filter pad material (Model HPE30651 Electrostatic Hammock filter pad, True Blue Company, Indiana, USA), galvanized ducts and rubber tubing. Figure 3.3 shows the schematic diagram and a photograph of the set-up.

The centrifugal fan was used to create the flow of gases through the adsorption column by extracting the headspace gases from the manure containers. The adsorption column was made of clear cylindrical PVC tubing with internal diameter and height of 7.5 cm and 25 cm, respectively. A layer of filter material was placed at the bottom of the column to hold the nanoparticles in the column. A filter screen made up of metallic mesh, glass wool, 0.6 cm spherical beads and filter material was placed at the top of the column to prevent the nanoparticles from blowing out of the column. The column was connected to the manure containers using 10 cm flexible rubber tubing and to the centrifugal fan using 10 cm galvanized ducts. Two sampling ports were installed before and after the adsorption column to collect influent and effluent gas samples for analysis. The gas flow rate was controlled by adjusting a damper at the exhaust of the centrifugal fan and with vents installed on the galvanized duct upstream of the fan. A thermal anemometer was used to measure the gas flow rate. The manure containers had a cover with an outlet connected to the adsorption column by the flexible rubber tubing. A stirrer was also fixed at the top of the container to agitate the manure during the tests. About 68.5 g of ZnO nanoparticles with 18 nm particle size, amounting to about 2.54 cm in bed depth, were used for the tests; this particle size was shown during the laboratory tests to be more effective in H_2S adsorption than 80-200 nm nanoparticles.

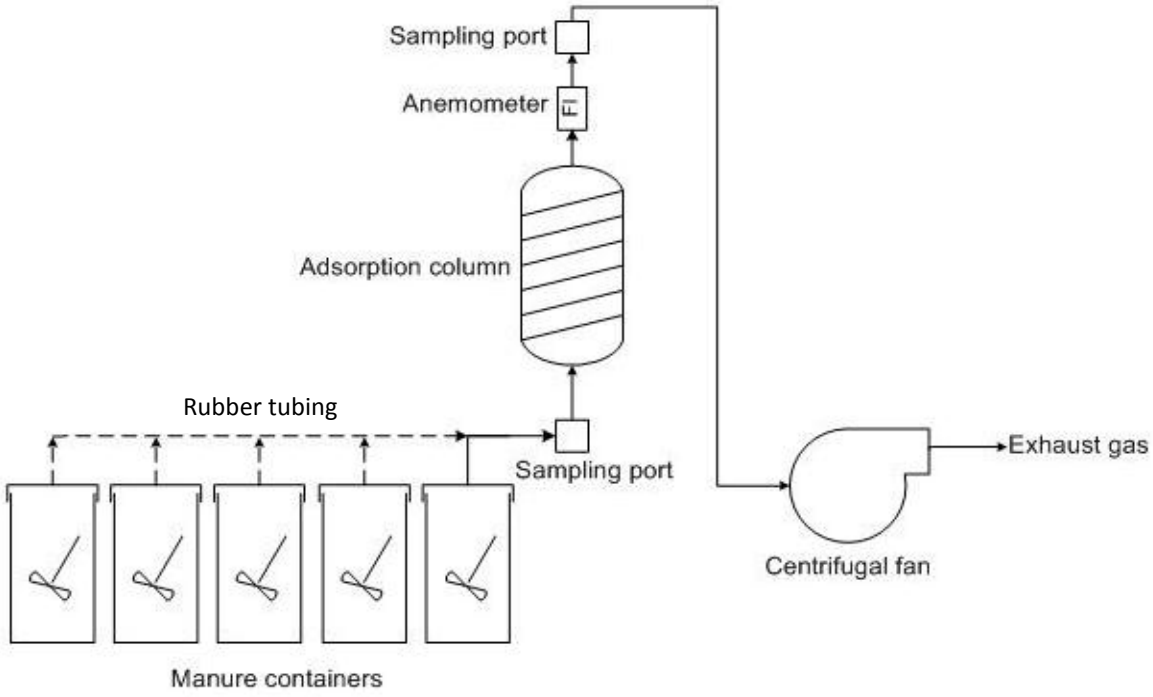

A

B

Figure 3.3. Schematic diagram (A) and photo (B) of the semi-pilot scale experimental set up.

3.4.2. Experimental procedures

The experiment was designed to simulate the actual gas concentration profiles that occur in swine barns when manure is agitated during manure pit drainage and high gas concentrations are generated for relatively short periods. This was achieved using 5 containers partially filled with the swine manure to generate manure gas for ~100 minutes (20 minutes for each manure container). The manure in the containers was agitated for a period of 2 minutes at the start of the run and then every 5 minutes. After the 20-minute period, the flexible tubing connection was moved to the next manure container and the same procedure was repeated. Prior to the start of the run, the adsorption column was filled with 2.54 cm (68.5 g) of nanoparticles and clean air was used to test the system for leakages and the flow rate was set at 25 L s^{-1}, which was established in preliminary tests to be the level that completely fluidized the adsorption bed. The first gas samples were taken after 2 minutes of agitation and at 5 minutes interval for subsequent samples. The samples were taken at both the influent and effluent sampling ports at each sampling event. The gas samples were taken using 20 ml air tight gas syringes and transferred into sampling tubes maintained under reduced pressure. Duplicate samples were taken occasionally to verify the accuracy of the results. Gas samples were also collected in 10-L Tedlar® gas sampling bags with a septum-embedded cap (SKC Inc., Eighty Four, PA, USA) to compare with sampling tube results. The gas samples were collected in the Tedlar bags using a gas sampling apparatus that consisted of an air tight container with 1 pump outlet and 4 sampling ports. The sampling apparatus was operated using the lung principle wherein a pump (Master flex L/S tubing pump, Model 7012-52 pump head, Vernon Hills, USA) was connected to the pump outlet to create negative pressure in the container, thereby drawing in gas stream through the sampling ports and filling the Tedlar bags attached to the sampling ports inside the container. Two Tedlar bags were filled with gas samples from the influent and effluent sampling ports on the set-up. Gas samples in the sampling tubes and Tedlar bags were taken to the laboratory for GC analyses.

A second test was conducted 2 weeks later to assess the reproducibility of the results obtained in the first test. In this test, three manure containers were used to generate manure gas (~25 minutes from each container). Nanoparticles used in this experiment were the same ones used in the previous test (i.e. they were not regenerated nor replaced). The experimental procedure was

carried out in the same way as the first experiment. Gas samples were taken from both the influent and effluent sampling ports at 3-5 minutes intervals. The manure was agitated for 2 minutes before gas samples was taken to generate measurable amount of H_2S. In addition to H_2S, concentration of NH_3 in the collected samples was also determined to assess the effectiveness of ZnO nanoparticles in adsorption of NH_3. The third manure container was used to run a control test without nanoparticles to check for potential adsorption by any part of the set-up.

3.5. Analysis

The level of H_2S in the influent and effluent was determined using a Varian CP-3800 gas chromatograph (GC) equipped with pulsed flame photometric detector (PFPD) and a capillary column (GS-GasPro 30 m x 0.32 mm I.D., Agilent Technologies). The carrier gas was ultra-purity grade nitrogen at a flow rate of 2.0 mL min^{-1}. The column oven temperature used throughout each run was 150 °C. Gases containing 0.2, 0.5, 1.24, 19.4, 98, 200, 500, 1000 and 1954 mg H_2S L^{-1}, balanced with nitrogen (Praxair, Saskatoon, Canada) were used to calibrate the GC. Three calibration curves (0.2-19.4, 19.4-500, 500-1954 mg H_2S L^{-1}) were generated and each of them had R^2 values greater than 99%. The split ratios (N_2:H_2S sample) used were 1:2, 1:80 and 1:150, respectively. The gas samples were analysed at least twice to check for reproducibility of the results. A calibration gas was injected before, in the middle and after each experimental run to ensure the accuracy of the results.

The level of NH_3 in the contaminated (influent) and treated gas (effluent) was determined using an ammonia analyzer (Model Chillgard RT, MSA Canada, Edmonton, AB). The analyser was connected to the sampling bags using 0.4 cm Teflon tubing. Standard NH_3 gases were used to calibrate the analyzer and to ensure the accuracy of the results.

4. RESULTS AND DISCUSSION

4.1. Laboratory scale experiments

As indicated in section 3.3.3, breakthrough curves were generated by plotting $\frac{C}{Co}$ versus time (where C is effluent concentration and Co is influent) to study the effects of feed concentration, nanoparticles size, temperature, feed gas flow rate and adsorbent quantity on H_2S adsorption on ZnO nanoparticles. The slope of the breakthrough curves is representative and proportional to how fast the adsorbent reaches saturation state. When comparing different breakthrough curves, a steeper curve indicates that adsorbent reaches saturation state in a relatively shorter period.

4.1.1. Effect of feed H_2S concentration

To study the effect of feed H_2S concentration on adsorption, experiments were performed using feed H_2S concentrations of 94.70, 233.43, 540.60, 814.76, 964.2 and 1501.85 mg L^{-1}. Experiments were conducted using 18 nm ZnO nanoparticles at constant flow rate of 200±0.2 mL min^{-1} and 22±1 ˚C. Duplicate experimental runs (shown in the appendix A) were performed for feed concentration of 964.2 and 1501.85 mg L^{-1} and the highest standard deviation recorded for $\frac{C}{C_0}$ were 0.19 and 0.09, respectively. As shown in Figure 4.1A, the adsorbent reached saturation state faster as the concentration of H_2S in the feed stream was increased (i.e. the steepness of the slope at lower feed concentration range increased dramatically, when the concentration of hydrogen sulphide in the feed stream was increased from 94.7 to 540.6 mg L^{-1}). A similar dependency was also observed at higher H_2S concentration range of 814.76 to 1501.85 mg L^{-1}, though variation in the slope of the breakthrough curve was less drastic in this case (Figure 4.1B). The breakthrough times decreased from 184.2 to 13.1 minutes as the feed concentration increased from 94.70 mg L^{-1} to 1501.85 mg L^{-1}. These could be explained by the fact that as the concentration of H_2S is increased in the feed stream, the driving force for mass transfer along the pores is enhanced. Thus, the breakthrough curves are steeper and the equilibrium is reached faster. At low feed concentrations, the driving force is lower so mass transfer is enhanced by the large volume of gas that comes in contact with the adsorbent surface. Also, a given mass of the adsorbent is able to take up a particular quantity of H_2S before it gets saturated, therefore, with the higher concentrations the adsorbent captures much H_2S faster and gets saturated faster (Xiao et al., 2008). The change in bed temperature recorded during the

adsorption process was ±1 ˚C. Also, the pressure drop across the adsorption bed was 0.68±0.20 kPa, which was negligible.

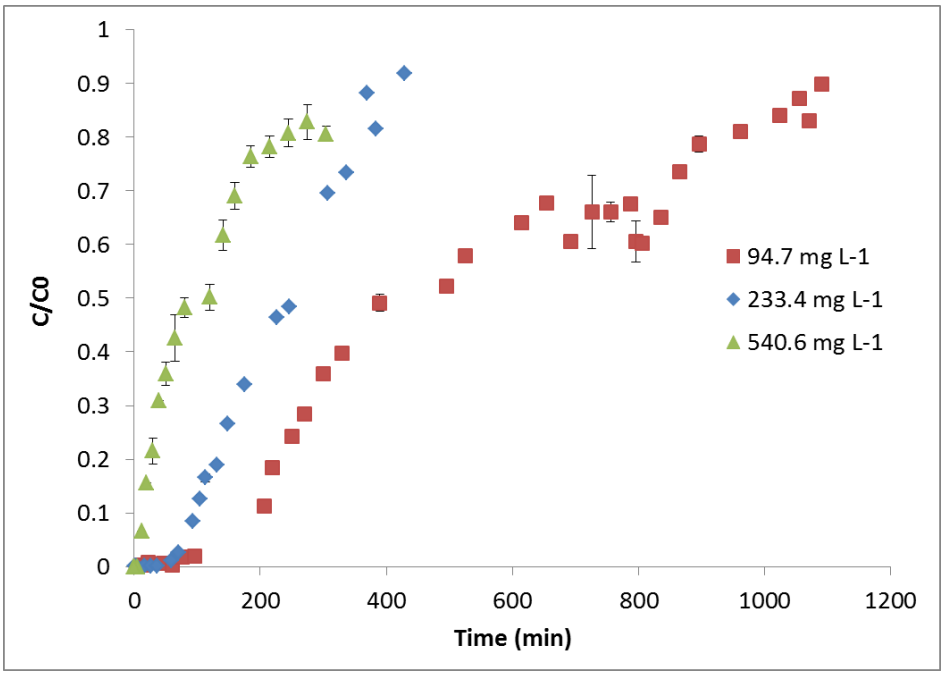

A

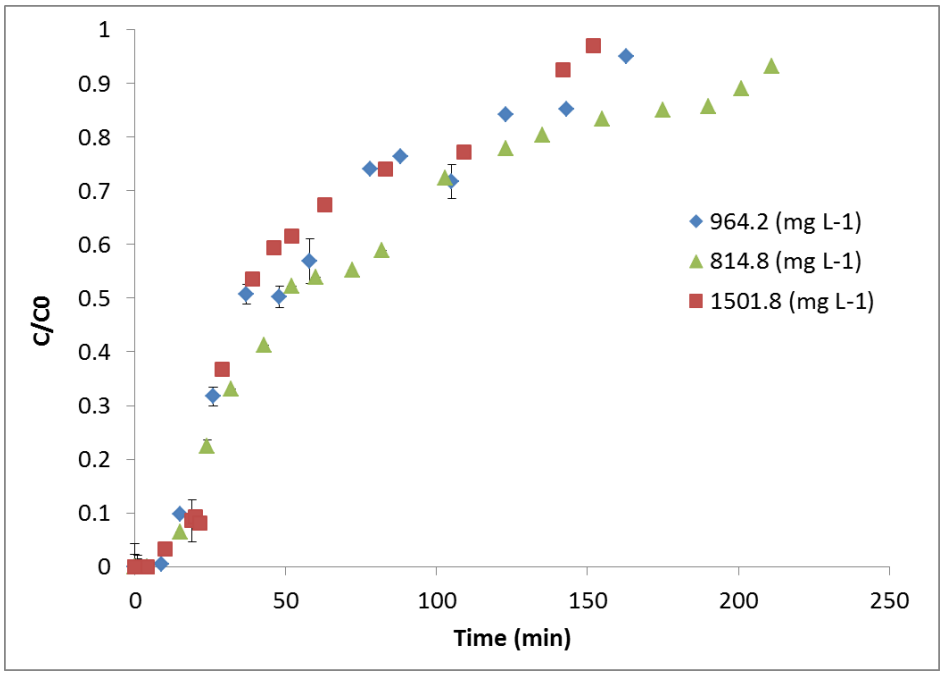

B

Figure 4.1. Breakthrough curves for H_2S adsorption on ZnO nanoparticles (18 nm) for feed H_2S concentrations of 94.7, 233.4 and 540.6 mg L^{-1} (A); and 814.8, 964.2 and 1501.8 mg L^{-1} (B).

The breakthrough adsorption capacity of the bed was calculated and the values for feed H_2S concentrations of 94.70, 233.43, 540.60, 814.76, 964.2 and 1501.85 mg L^{-1} were 0.10, 0.14, 0.06, 0.07, 0.10 and 0.13 g adsorbed H_2S (g adsorbent)$^{-1}$, respectively. This shows that the breakthrough adsorption capacity was not affected drastically by the change in feed H_2S concentration. The equilibrium adsorption capacity of the nanoparticles for feed H_2S concentrations of 94.70, 233.43, 540.60, 814.76, 964.2 and 1501.85 mg L^{-1} were 9.2, 9.8, 10.6, 10.6, 11.4, and 14.9 g H_2S adsorbed (g adsorbent)$^{-1}$, respectively. The equilibrium adsorption capacity of the bed increased with increased feed H_2S concentration.

Xiao et al. (2008) investigated the effect of feed concentration on the adsorption of H_2S on sodium carbonate impregnated activated carbon and untreated activated carbon. They recorded an increase from 0.0021 to 0.0030 g H_2S adsorbed (g adsorbent)$^{-1}$ with sodium carbonate impregnated activated carbon when feed concentration was increased from 200 to 1000 mg L^{-1}, and an increase from 0.0077 to 0.0093 g H_2S adsorbed (g adsorbent)$^{-1}$ with untreated activated carbon when feed concentration was increased from 200 to 1000 mg L^{-1}. The results showed an increase in equilibrium adsorption capacity with increase in feed concentration. Rosso et al. (2003) investigated the removal of H_2S by synthesized ZnO nanoparticles using feed H_2S concentration of 100 mg L^{-1} and feed flow rate of 400 mL min^{-1} at 250 ˚C. They reported that the breakthrough adsorption capacities for ZnO300 (surface area - 50.3 m^2/g) and ZnO400 (surface area - 43.3 m^2/g) were 0.03 and 0.02 g H_2S adsorbed (g adsorbent)$^{-1}$, respectively. The equilibrium adsorption capacities for ZnO300 and ZnO400 adsorbents were both 0.051 g H_2S adsorbed (g adsorbent)$^{-1}$. It was also reported that the internal mass transfer resistance was the limiting factor in the adsorption process (Rosso et al., 2003). The characteristics of the nanoparticles and different experimental conditions could account for the high adsorption capacities reported in this work. Higher H_2S concentrations ranges (94.70 mg L^{-1} to 1501.85 mg L^{-1}) were used in this work. The surface area of the 18 nm ZnO nanoparticles ranged between 40 to 70 m^2g.

A similar increasing trend of the slope in the breakthrough profiles was observed with increase in the feed concentration when 80-200 nm nanoparticles were used (shown in Figure 4.2). The breakthrough adsorption capacity of the bed was calculated and the values at feed H_2S

concentrations of 86.81, 202.14, 345.03, 515.80, 1033.33 and 1523.55 mg L^{-1} were 0.002, 0.006, 0.008, 0.010, 0.14 and 0.18 g adsorbed H_2S (g adsorbent)$^{-1}$, respectively. The corresponding equilibrium adsorption capacity values were 1.7, 2.5, 3.9, 4.0, 4.7, and 6.0 g H_2S adsorbed (g adsorbent)$^{-1}$, respectively. The explanation for the increasing slope trend and adsorption capacities with increase in feed concentration is the same as that of the 18 nm nanoparticles described above.

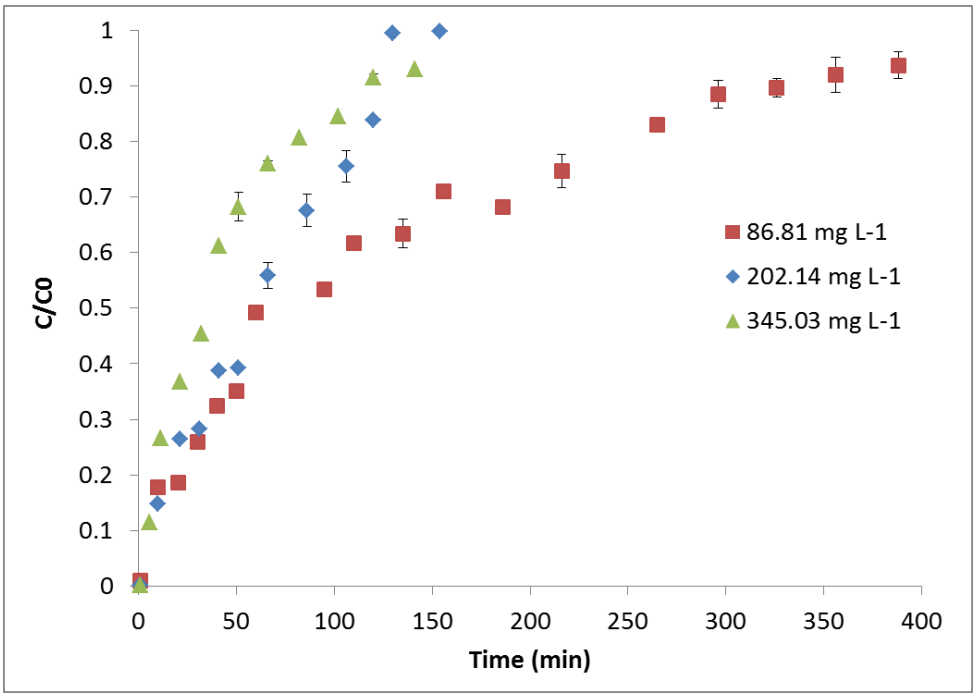

A

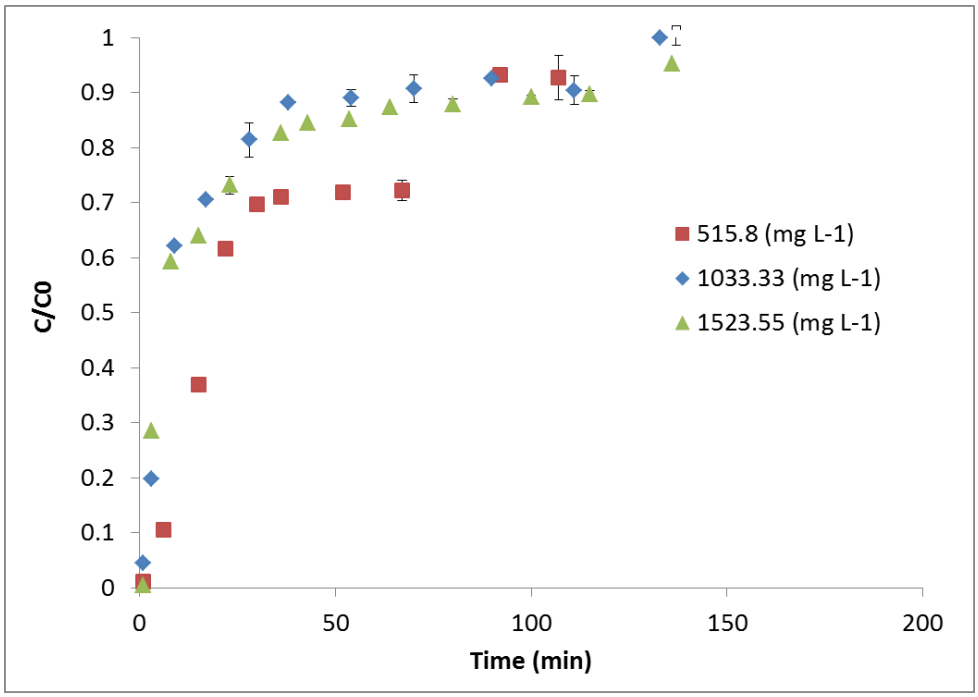

B

Figure 4.2. Breakthrough curves for H_2S adsorption on ZnO nanoparticles (80-200 nm) for feed H_2S concentrations of 86.81, 202.14 and 345.03 mg L^{-1} (A); and 515.80, 1033.33 and 1523.55 mg L^{-1} (B).

4.1.2. Effect of nanoparticles size

The effect of particle size on H_2S adsorption was studied by comparing the results from experiments performed with 18 and 80-200 nm nanoparticles at different feed concentrations. The experimental conditions were kept constant for the two sets of experiment (i.e. gas flow rate: 200 ml min^{-1}; and temperature: 22±1˚C). As seen in Figure 4.3, comparison between breakthrough curves for 18 and 80-200 nm using feed H_2S concentration of 94.70 and 86.80 mg L^{-1} (A), 233.43 and 202.14 mg L^{-1} (B), 540.60 and 515.80 mg L^{-1} (C), 964.19 and 1033.33 mg L^{-1} (D), 1501.85 and 1523.55 mg L^{-1} (E), respectively show that the curves are steeper for the bigger nanoparticles. Hence, for larger particle size, the nanoparticles reached saturation state faster. Interestingly, this trend was observed for all the tested feed concentrations. The nanoparticles size affected the slope of breakthrough profiles, indicating that the smaller nanoparticles which provided a higher surface area reached their saturation state after a longer period compared to the larger nanoparticles. The slope of the breakthrough curve is affected by macropore diffusion. Simo (2009) indicates that the breakthrough curve will not change if the macropore diffusion is negligible. Macropore diffusional resistance occurs within the bulk crystalline structure of the solid phase. This resistance can be reduced when the bulk particle size is smaller.

The breakthrough adsorption capacity of the 18 nm ZnO nanoparticles was calculated and the values at feed H_2S concentrations of 94.70, 233.43, 540.60, 964.2 and 1501.85 mg L^{-1} were 0.10, 0.14, 0.06, 0.10 and 0.13 g adsorbed H_2S (g adsorbent)$^{-1}$, respectively. The value for 80-200 nm ZnO nanoparticles at feed H_2S concentrations of 86.81, 202.14, 515.80, 1033.33 and 1523.55 mg L^{-1} were 0.002, 0.006, 0.010, 0.14 and 0.18 g adsorbed H_2S (g adsorbent)$^{-1}$, respectively. When the breakthrough adsorption capacities at the same feed concentrations are compared, it becomes clear that the values for the 18 nm ZnO particles were higher. The same increasing trend was observed when the equilibrium adsorption capacities were calculated and compared. The equilibrium adsorption capacity of the 18 nm nanoparticles for feed H_2S concentrations of 94.70, 233.43, 540.60, 964.2 and 1501.85 mg L^{-1} were 9.2, 9.8, 10.6, 11.4, and 14.9 g H_2S adsorbed (g adsorbent)$^{-1}$, respectively. The values for 80-200 nm nanoparticles at feed H_2S concentrations of 86.81, 202.14, 515.80, 1033.33 and 1523.55 mg L^{-1} were 1.7, 2.5, 4.0, 4.7, and 6.0 g H_2S adsorbed (g adsorbent)$^{-1}$, respectively. No significant change was observed in bed temperature during the tests. Also, a small pressure drop of 0.68±0.20 kPa was recorded.

Novochinskii et al. (2004) evaluated the effect of particle size on H_2S adsorption on ZnO. They reported a decrease in breakthrough adsorption capacity from 0.0041 to 0.0023 H_2S adsorbed (g adsorbent)$^{-1}$ as the particle size was decreased from 3 to 0.053-0.075 mm, respectively. These authors, however, indicated that the adsorption capacity was not affected when 0.053-0.075 mm particles were used, and that the probable limitation to adsorption of H_2S on ZnO was diffusion.

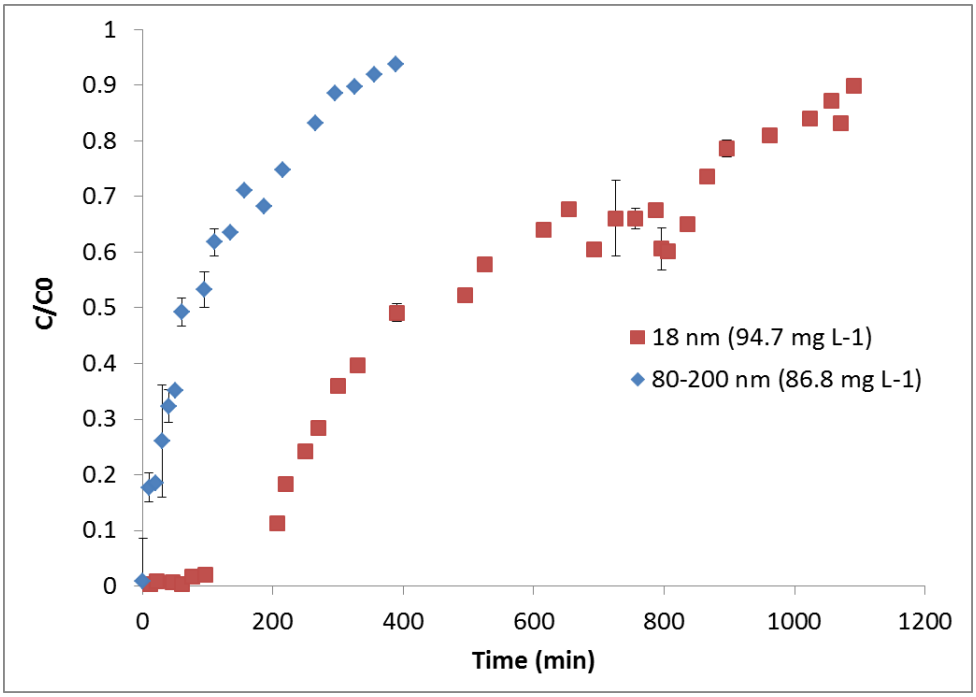

A

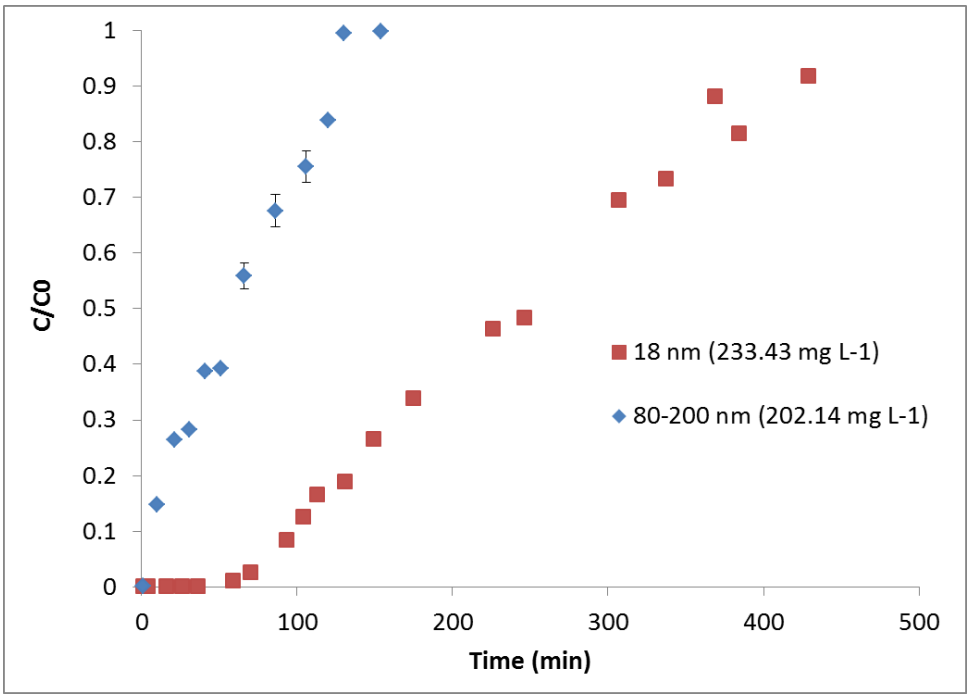
C/C0
Time (min)
18 nm (233.43 mg L-1)
80-200 nm (202.14 mg L-1)

B

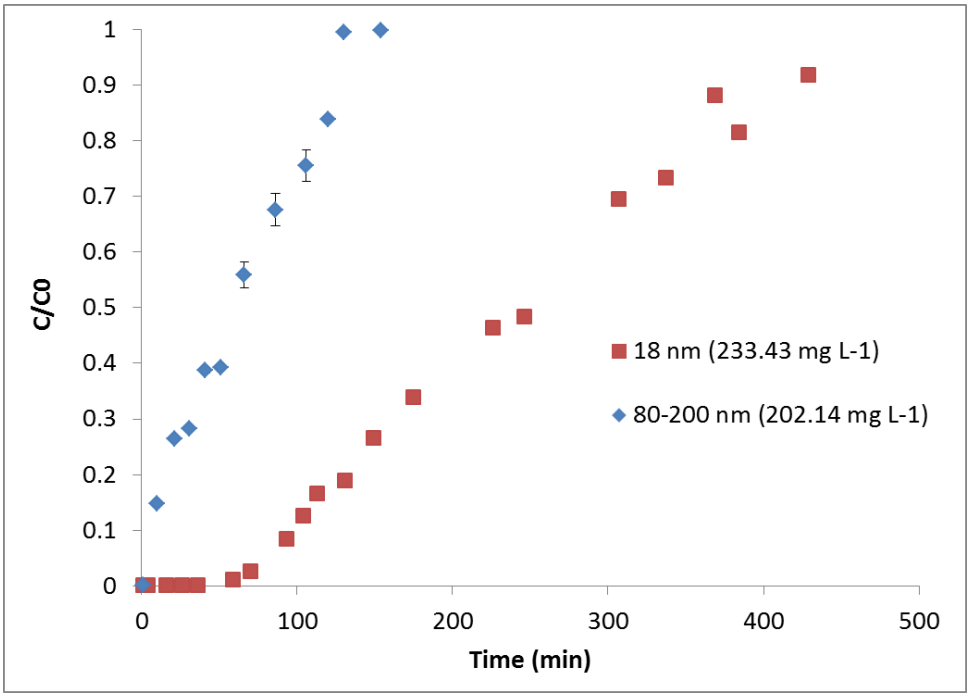
C/C0
Time (min)
18 nm (233.43 mg L-1)
80-200 nm (202.14 mg L-1)

C

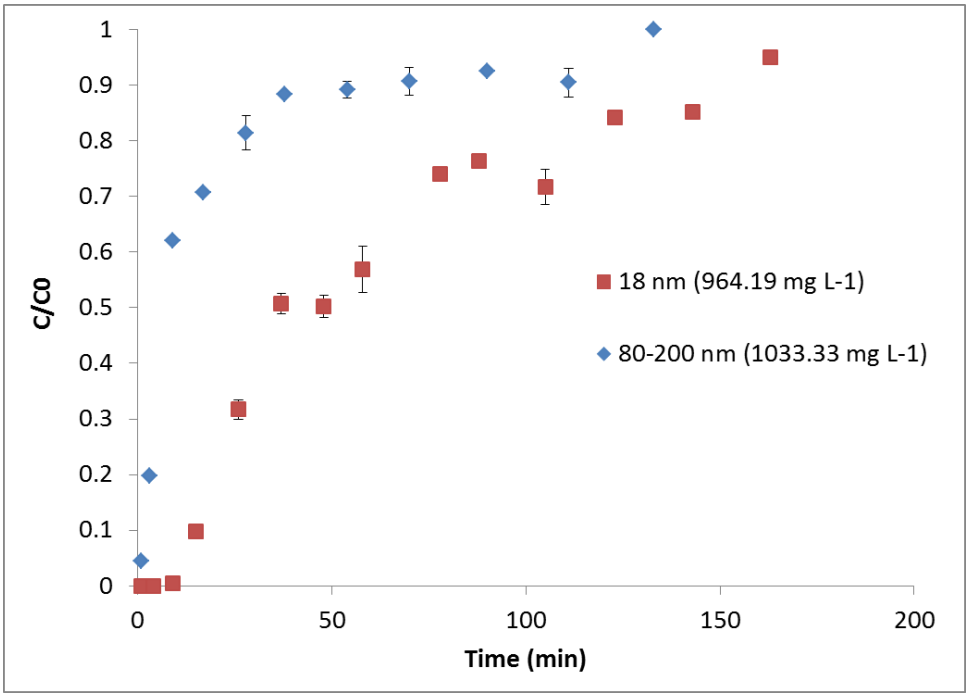

D

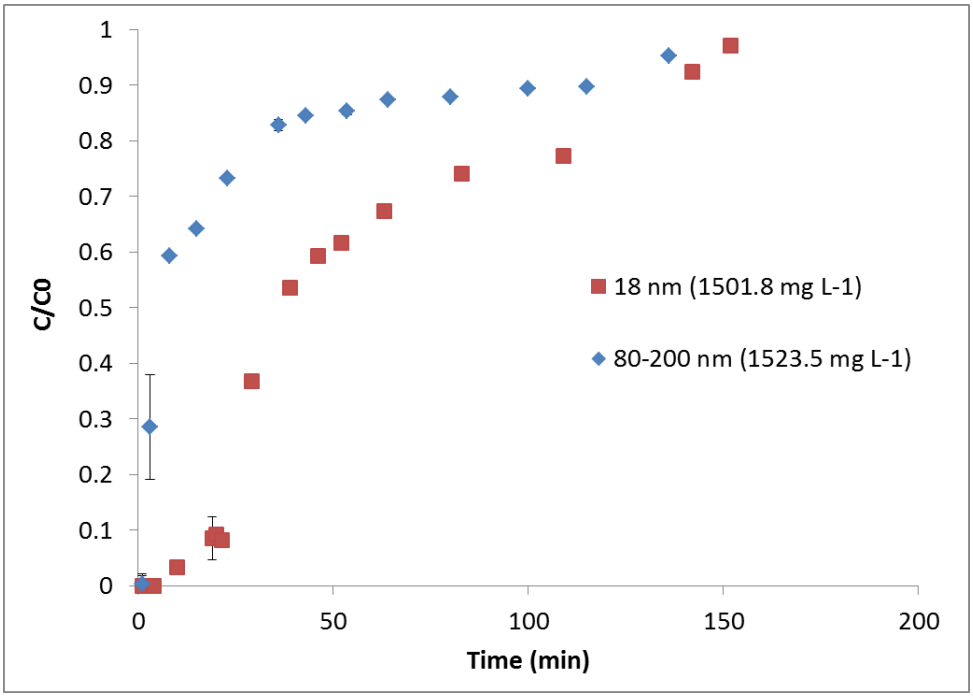

E

Figure 4.3. Breakthrough curves for H_2S adsorption on 18 and 80-200 nm ZnO at feed H_2S concentrations of 94.70 and 86.80 mg L^{-1} (A); 233.43 and 202.14 mg L^{-1} (B); 540.60 and 515.80 mg L^{-1} (C); 964.19 and 1033.33 mg L^{-1} (D); and 1501.85 and 1523.55 mg L^{-1} (E).

4.1.3. Effect of gas flow rate

To study the effect of feed gas flow rate on H_2S adsorption, an additional experimental run was performed using a feed flow rate of 450±0.3 mL min^{-1}. These runs were performed using 18 nm nanoparticles at 22±1˚C and the results were compared with earlier test performed using feed gas flow rate of 200±0.2 mL min^{-1}. The breakthrough curves shown in Figure 4.4 indicates that the nanoparticles reached saturation state faster as the feed gas flow rate was increased. There were no significant changes in the bed temperature and the pressure drop was negligible. Simo (2009) notes that the external mass transfer process is directly dependent on the superficial velocity of the gas (flow rate of the gas). The saturation state was reached faster for the high feed flow rate because the increase in gas flow rate decreased the external mass transfer resistance (Simo 2009).

The breakthrough adsorption capacity calculated for test with feed flow rate of 200±0.2 and 450±0.3 mL min^{-1} were 0.14 and 0.16 g H_2S adsorbed (g adsorbent)$^{-1}$, respectively. The corresponding equilibrium adsorption capacity values were 10.6 and 11.1 g H_2S adsorbed (g adsorbent)$^{-1}$, respectively. This shows that flow rate did not significantly affect the adsorption capacities. Slight increases were observed but these could be due to experimental errors. Some studies, however, showed a decrease in adsorption capacities with increase in gas flow rate. Habibi et al. (2010) examined the effect of gas hourly space velocity (GHSV) on H_2S adsorption on rod-like nano-ZnO. They recorded breakthrough capacity values of 0.2401 and 0.0731 g H_2S adsorbed (g adsorbent)$^{-1}$ for space velocities of 4000 and 8000 h^{-1}, respectively. The reason was that with lower flow rates there was more time for the H_2S gas to react with the ZnO nanoparticles. Li et al. (2006) also reported a decrease in adsorption capacity with increase in gas flow rate. The differences in the experimental conditions used make it impractical to compare the results to these and present work.

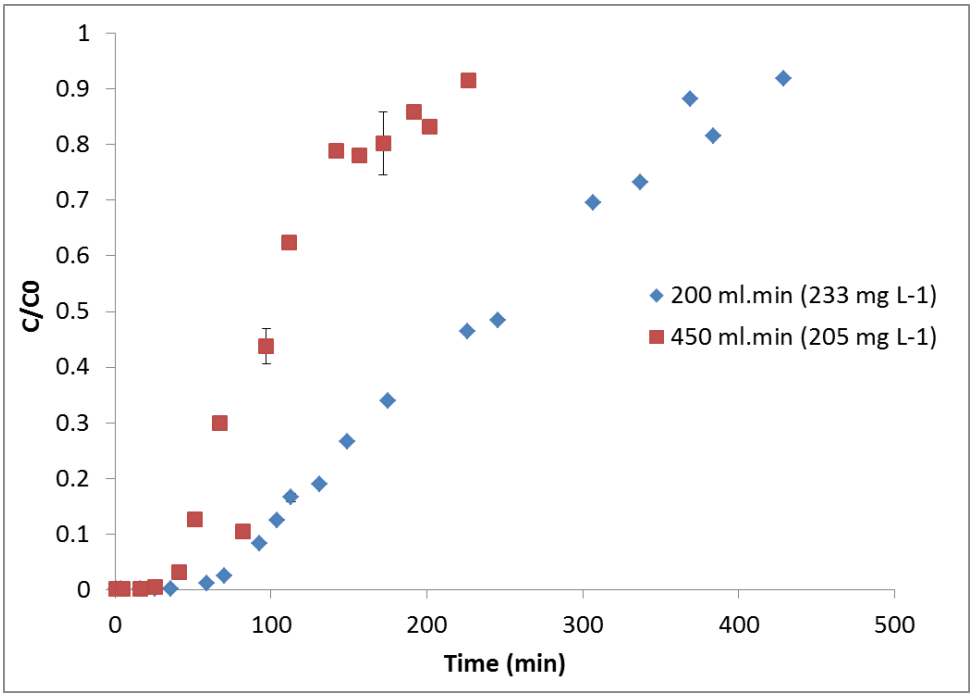

Figure 4.4. Breakthrough curves for H_2S adsorption on ZnO nanoparticles (18 nm) for feed H_2S concentrations of 200±33 mg L^{-1} showing feed flow rates of 200±0.2 mL min^{-1} and 450±0.3 mL min^{-1}.

4.1.4. Effect of temperature

The effect of temperature on the adsorption of 541.4±4.3 mg L^{-1} and 1567.8±63.0 mg L^{-1} H_2S was studied using 18 nm ZnO nanoparticles and a feed gas flow rate of 200±0.2 mL min^{-1}. As shown in Figure 4.5, the slope of the curve in both sets of tests was slightly steeper when the temperature was decreased. The breakthrough adsorption capacities at feed H_2S concentration of 541.4±4.3 mg L^{-1} at 1, 11, 22, and 41˚C were 0.04, 0.07, 0.06, and 0.06 g H_2S adsorbed (g adsorbent)$^{-1}$, respectively. These did not change significantly when temperature was increased. There was, however, a decrease in the breakthrough capacity as temperature increased at feed concentration of 1567.8±63.0 mg H_2S L^{-1}. The calculated values at 11, 22, and 41˚C were 0.19, 0.13, and 0.07 g H_2S adsorbed (g adsorbent)$^{-1}$, respectively.

The equilibrium adsorption capacity for feed H_2S gas concentration of 541.4±4.3 mg L^{-1} at 1, 11, 22, 41˚C was 8.35, 9.21, 10.58, 11.17 g H_2S adsorbed (g adsorbent)$^{-1}$, respectively. The values for feed H_2S gas concentration of 1567.8±63.0 mg L^{-1} at 11, 22, and 41˚C were 12, 14.9 and 16.6

g H_2S adsorbed (g adsorbent)$^{-1}$. These indicate an increase in the equilibrium adsorption capacities for both sets of tests with increase in temperature. According to Simo (2009), micropore diffusion has a strong dependence on temperature, while macropore diffusion is not affected by temperature to the same extent. The results from this work show that the change in temperature did not affect the adsorption rate because the micropore mass transfer did not limit adsorption at the range of temperatures studied. Nassar and Pereira-Almao (2010) however recorded an increase in the slope of the breakthrough curves as temperature was increased from 25 to 200 ˚C when they examined the effectiveness of different metal oxides (ZnO, Al_2O_3, NiO and CuO) on H_2S adsorption. Habibi et al. (2010) investigated H_2S adsorption using nano-zinc oxide (rodlike and spherical morphology) at a feed flow rate of 1100 mL min^{-1}. The breakthrough adsorption capacity reported for rod-like ZnO nanoparticle at 150 and 250 ˚C were 0.20 and 0.24 g H_2S adsorbed (g adsorbent)$^{-1}$, respectively. The reason for the differences in the temperature effect on breakthrough curve and capacities observed in the various studies may be due to the different characteristics of nanoparticles and experimental conditions used in these works. Feed H_2S concentrations ranges (94.70 mg L^{-1} to 1501.85 mg L^{-1}) were used in this work. The specific surface area of the 18 nm ZnO nanoparticles ranged between 40 to 70 m^2 g^{-1}. Also, ambient temperatures (1 – 11 °C) were used in this work.

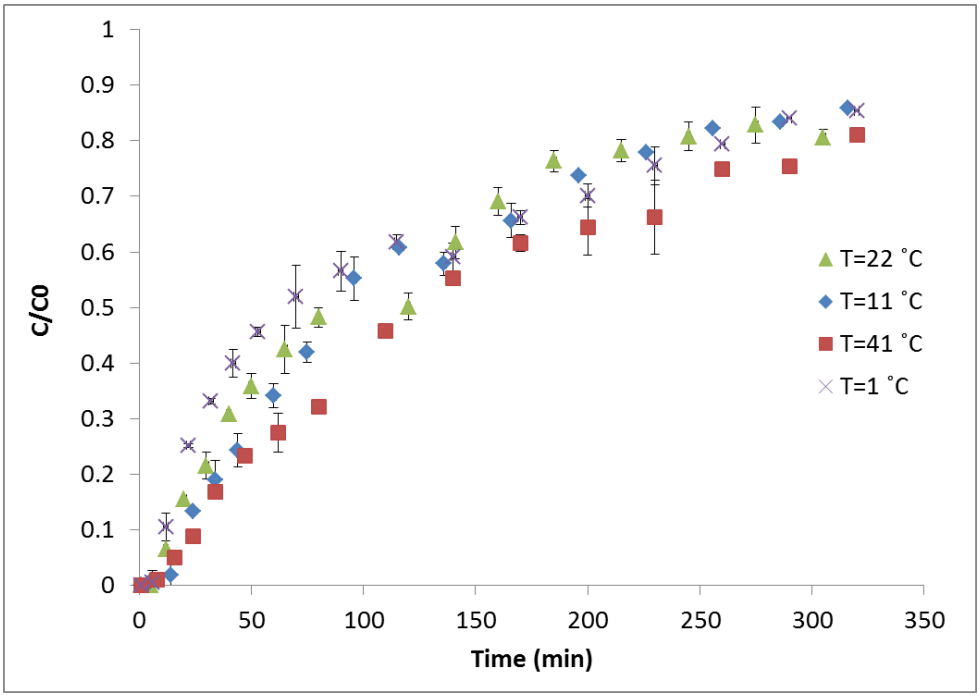

A

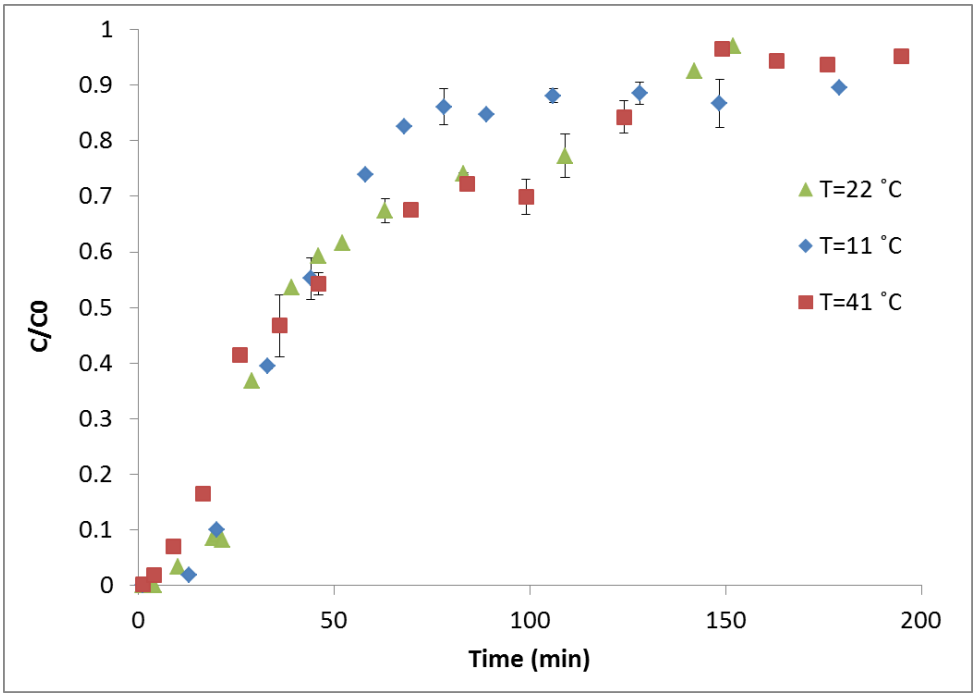

B

Figure 4.5. Breakthrough curves for H_2S adsorption on ZnO nanoparticles (18 nm) showing profiles of feed H_2S concentration of 541.4±4.3 mg L^{-1} at 1, 11, 22, and 41˚C (A); and feed H_2S concentration of 1567.8±63.0 mg L^{-1} at 11, 22, and 41˚C.

4.1.5. Effect of adsorbent quantity

As described in section 3.3.2 of the experimental procedures, the effect of quantity of nanoparticles on H_2S adsorption was tested using feed H_2S concentrations of 1666.8 mg L^{-1} and 102.3 mg L^{-1}. These tests were carried out using 18 nm nanoparticles and a feed flow rate of 200±0.2 mL min^{-1} at 22±1˚C. The results for adsorption of 1666.8 mg H_2S L^{-1} on 0.5, 1 and 1.5 g of 18 nm ZnO nanoparticles, and 102.3 mg H_2S L^{-1} on 0.2, 0.5 and 1 g of 18 nm ZnO nanoparticles are shown in Figure 4.6 below. The breakthrough profiles show that the adsorbent reached saturation state faster when the nanoparticles quantity was reduced regardless of the feed H_2S concentration. This is as a result of the larger total surface area available for adsorption that the larger quantity of nanoparticles provided as compared to the smaller quantity.

The breakthrough adsorption capacity calculated for the experimental runs with feed H_2S concentration of 1666.8 mg L^{-1} were 0.04, 0.13, and 0.20 g H_2S adsorbed (g adsorbent)$^{-1}$ for 0.5, 1, and 1.5 g of ZnO nanoparticles, respectively. The values for the tests with 102.3 mg H_2S L^{-1} were 0.007, 0.027, and 0.099 g H_2S adsorbed (g adsorbent)$^{-1}$ for 0.2, 0.5, and 1 g ZnO nanoparticles, respectively. Both sets of tests show an increase in the adsorption capacities with increase in the quantity of ZnO nanoparticles. The equilibrium adsorption capacity calculated for the experimental runs with 1666.8 mg H_2S L^{-1} were 0.04, 0.13, and 0.20 g H_2S adsorbed (g adsorbent)$^{-1}$ for 0.5, 1, and 1.5 g ZnO, respectively. This shows a continued increasing adsorption capacity with increase in the ZnO nanoparticles quantity. However, when feed H_2S concentration of 102.3 mg L^{-1} was used, a relatively constant adsorption capacity of 9.2±0.2 g H_2S adsorbed (g adsorbent)$^{-1}$ was obtained.

Wang et al. (2008) investigated the removal of H_2S from gas streams using Mesoporous silica SBA-15 supported ZnO nanoparticles. They recorded that as the quantity of ZnO was increased from 0.50 wt % to 3.04 wt%, the breakthrough adsorption capacity increased from 0.036 to 0.436 g H_2S adsorbed (g adsorbent)$^{-1}$. The authors noted that small quantities of ZnO resulted in low efficiency in the removal of sulphur compound (Wang et al., 2008).

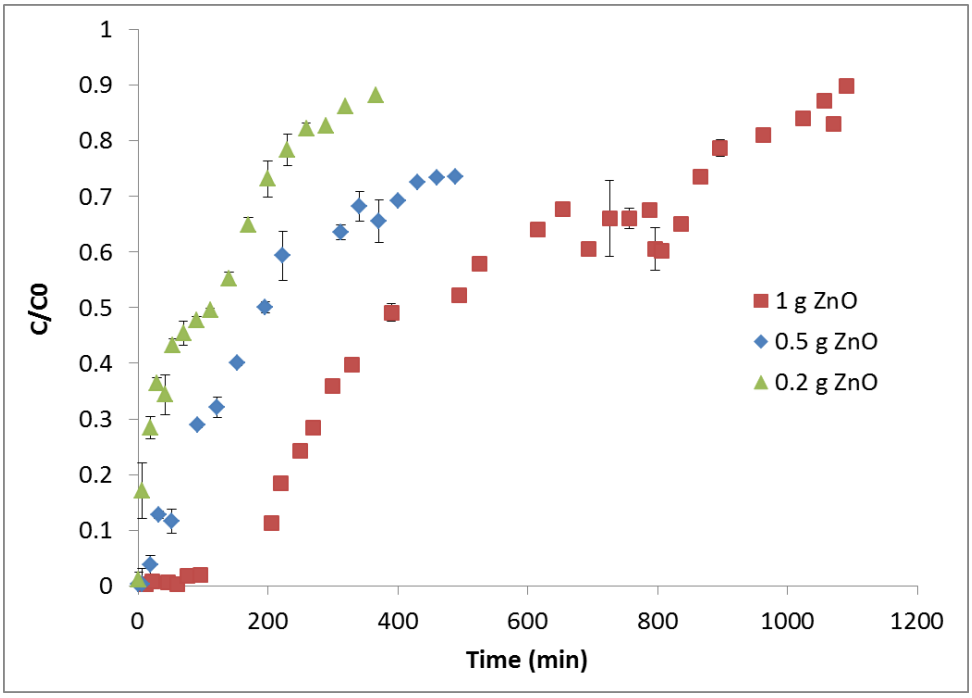

A

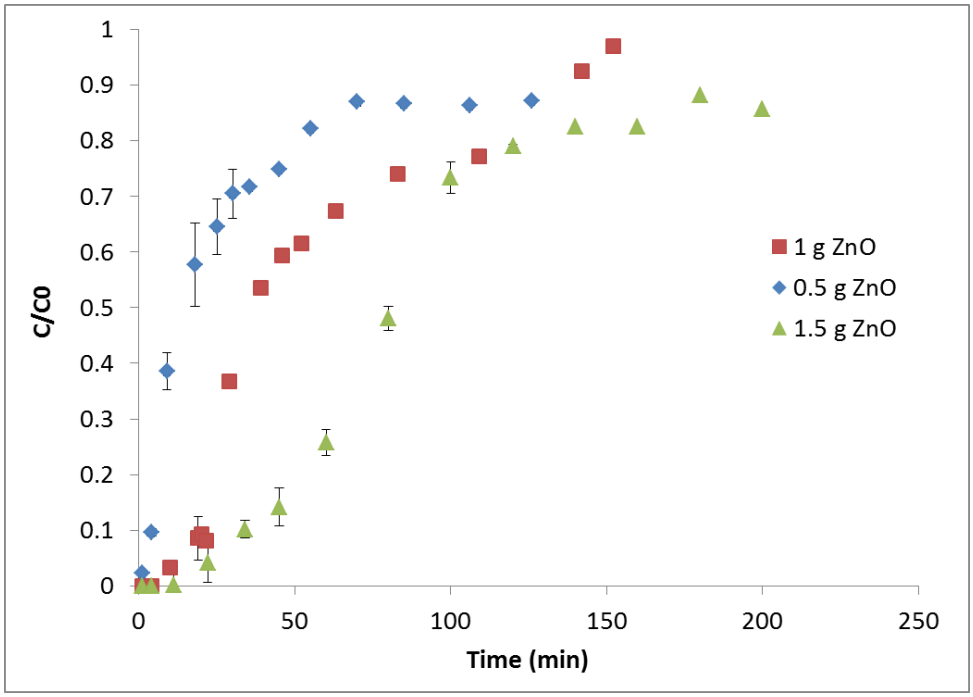

B

Figure 4.6. Breakthrough curves for H_2S adsorption on ZnO nanoparticles (18 nm) showing profiles of feed H_2S concentrations of 1666.8 mg L^{-1} using 0.5, 1, and 1.5 g of nanoparticles (A); and feed H_2S concentration of 102.3 mg L^{-1} using 0.2, 0.5, and 1 g of nanoparticles.

4.1.6. Adsorption isotherms

The experimental data were used to study the equilibrium adsorption of H_2S on ZnO nanoparticles and isotherms were generated by plotting the amount of H_2S adsorbed versus H_2S concentration at different temperatures. The equilibrium capacity of bed was calculated by integrating the area above the breakthrough curve for a given feed concentration and flow rate.

Figure 4.7 shows the adsorption isotherms for 3 sets of data: experiments performed at 10 and 22 °C using 18 nm ZnO nanoparticles, and at 22 °C using 80-200 nm ZnO nanoparticles. The data was fit into Langmuir, Freundlich, Langmuir- Freundlich and BET isotherms. As seen in Table 4.1, the BET isotherm gave the best fit for the data with a minimum coefficient of determination of 0.95. The isotherms show that, at constant temperature, the larger nanoparticles (80-200 nm) adsorbed less H_2S than the smaller nanoparticles (18 nm). Also, an increase in temperature within the range studied led to a decrease in the amount of H_2S adsorbed by the nanoparticles.

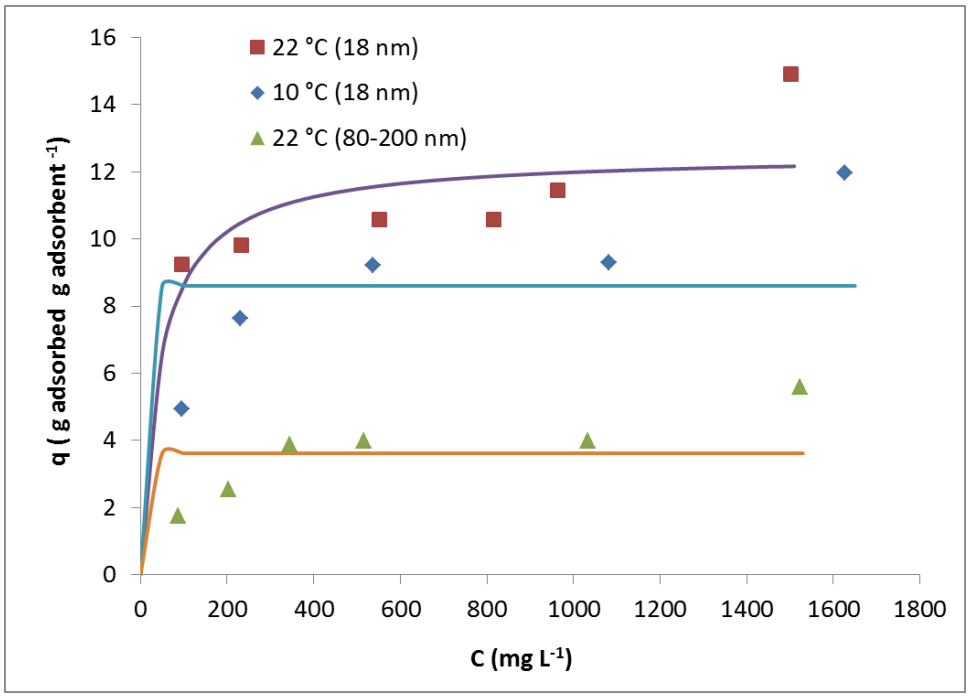

A

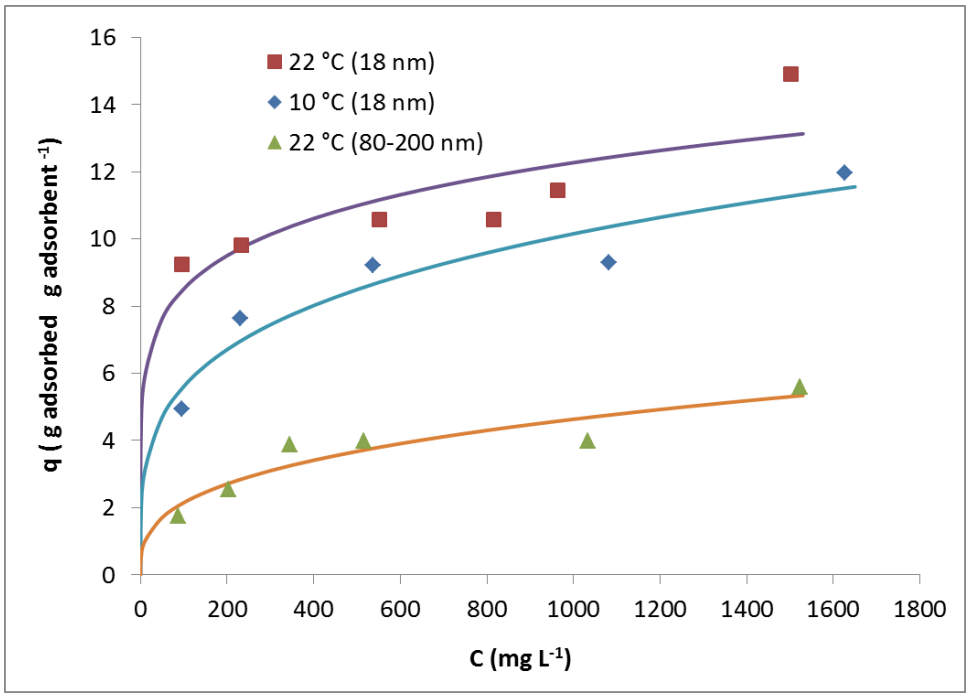
22 °C (18 nm)
10 °C (18 nm)
22 °C (80-200 nm)
q (g adsorbed g adsorbent -1)
C (mg L-1)
0
2
4
6
8
10
12
14
16
0
200
400
600
800
1000
1200
1400
1600
1800

B

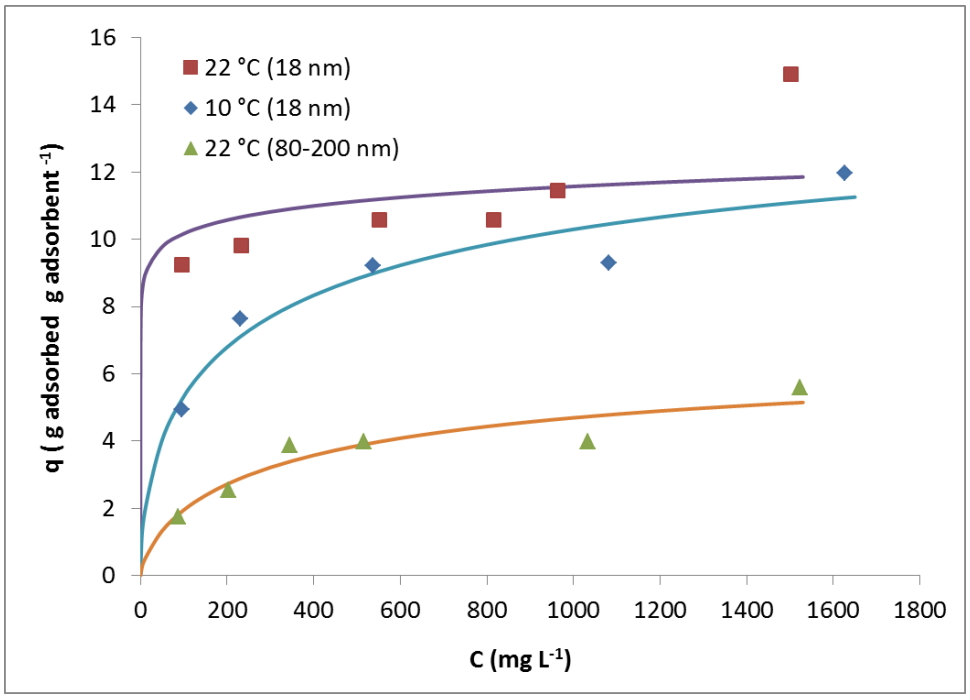
22 °C (18 nm)
10 °C (18 nm)
22 °C (80-200 nm)
q (g adsorbed g adsorbent -1)
C (mg L-1)
0
2
4
6
8
10
12
14
16
0
200
400
600
800
1000
1200
1400
1600
1800

C

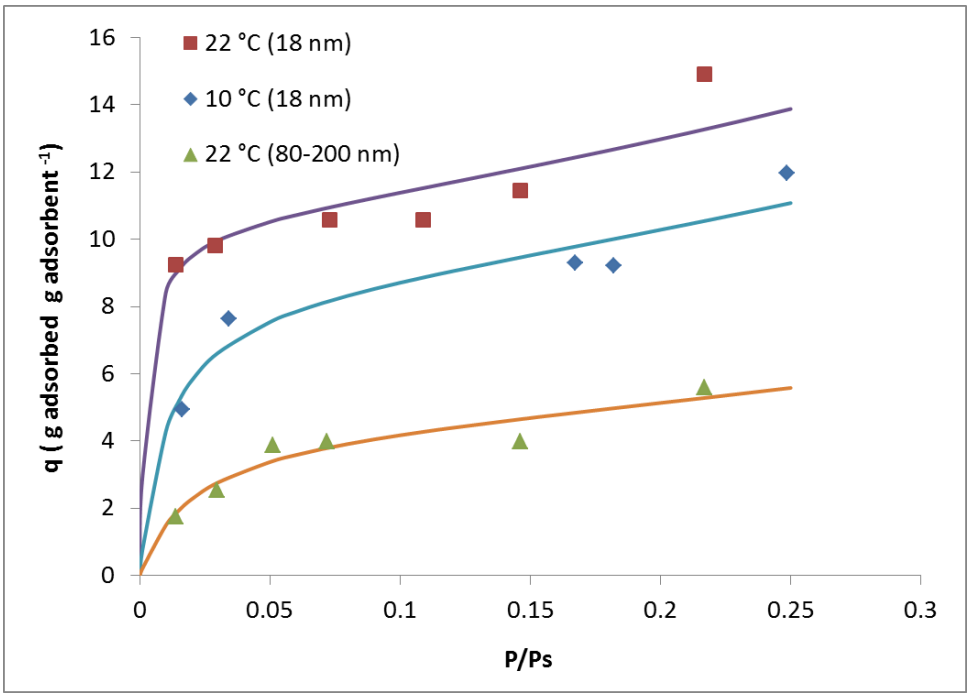

D

Figure 4.7. Langmuir (A), Freundlich (B) Langmuir-Freundlich (C) and BET (D) equilibrium isotherms of H_2S adsorption on ZnO nanoparticles (18 and 80-200 nm) at 10 and 22 °C.

Haimour et al. (2005) used isotherms to report the results for experiments done to investigate the removal of H_2S from aqueous solution using ZnO sorbent at 25 and 35˚C. They fitted the experimental data into Langmuir, Freundlich and Redlich-Peterson isotherms but reported that Redlich-Peterson isotherm gave a much better fit.

Table 4.2. Equilibrium isotherms and associated coefficients for H_2S adsorption on ZnO nanoparticles.

Isotherm model	T (˚C)	D_p (nm)	q_s (g H_2S adsorbed g adsorbent^{-1})	b	n	R^2
Langmuir	22	18	12.53	0.02	-	0.91
	10	18	8.60	-1889	-	0.70
	22	80-200	3.62	601.30	-	0.56
Freundlich	22	18	-	0.46	2.99	0.94
	10	18	-	1.71	3.88	0.97
	22	80-200	-	0.46	2.99	0.94
Langmuir-Freundlich	22	18	182.20	0.04	16.72	0.90
	10	18	15.67	0.03	1.75	0.97
	22	80-200	7.10	0.01	1.41	0.95
BET	22	18	10.49	381.80	-	0.97
	10	18	8.56	96.87	-	0.97
	22	80-200	4.44	49.46	-	0.95

(T - temperature, D_p - particle diameter, q_s - saturation limit, b and n - isotherm coefficients, R^2 - coefficient of determination)

4.2. Semi-pilot scale tests

Figure 4.8 shows the concentrations of H_2S in the feed and treated gas samples from the sampling ports installed on the semi-pilot scale setup. The average feed H_2S concentration recorded was 235.7±85.2 mg L^{-1}, with the lowest and highest concentrations being 139.9 and 366.6 mg L^{-1}, respectively. The 5 batches shown in Figure 4.8 show results from the tests with the 5 manure containers used. The variation in the feed concentration can be attributed to the variation in the collected manure samples and extent of anaerobic digestion in the stored manure, thereby leading to differences in the level of H_2S gas produced in each container. The pattern of feed H_2S gas profile extracted from each container, however, showed a similar pattern to that

observed in a typical barn setting during the processes involved handling of manure where high H_2S concentrations are measured within the first few minutes and then the concentration subsequently diminishes with time. An average H_2S concentration of 0.26 mg L^{-1} was recorded in the treated gas. This proves that the nanoparticles were able to effectively remove over 99% of the H_2S as it passed through the adsorption column regardless of the feed H_2S concentration.

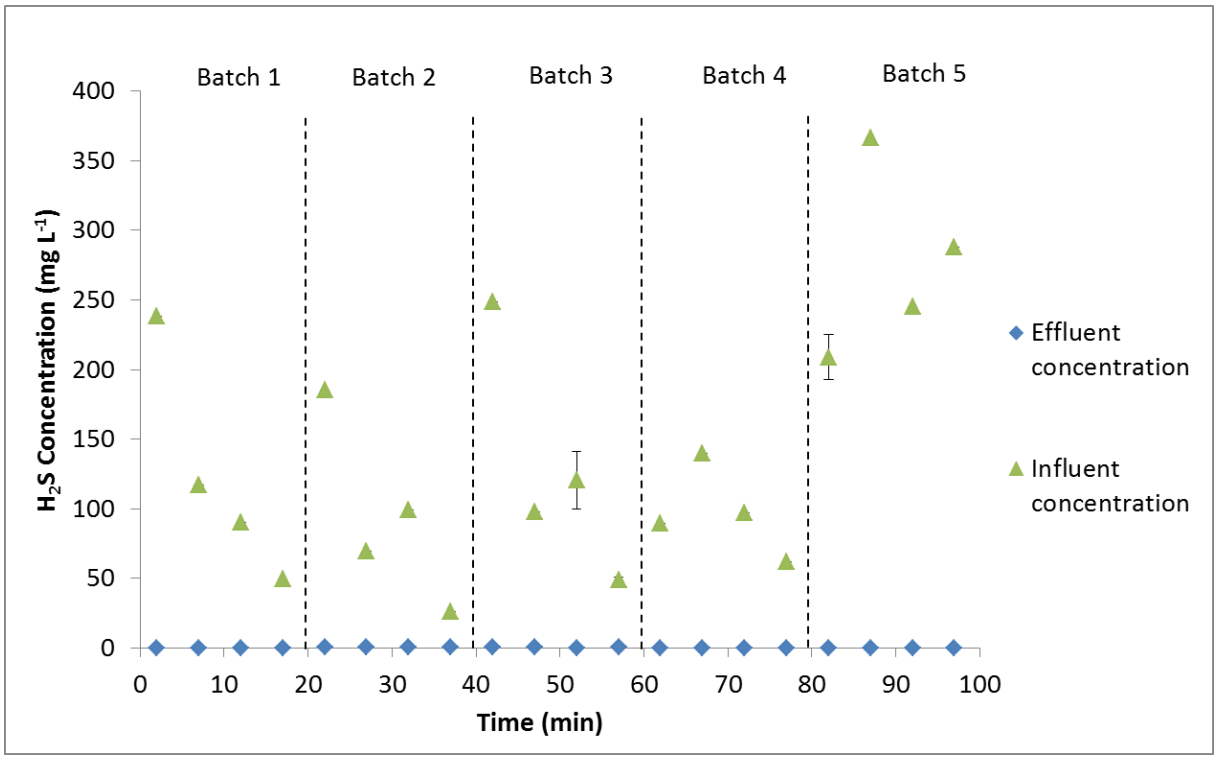

Figure 4.8. H_2S concentration profiles of the gases emitted from swine manure (influent gas) and treated gas (effluent gas).

As explained in the Materials and Methods (section 3.4.2), a second test was performed (results shown in Figure 4.9) 2 weeks after the first run to assess the reproducibility of the results. As compared to the first run, a lower average feed H_2S concentration of 60.92 mg L^{-1} was recorded. The difference is due to the variation in manure samples collected and the extent of anaerobic digestion in the stored manure. Again, as seen in Figure 4.9, the nanoparticles used in previous runs were able to remove more than 99% of the H_2S from the feed stream. The average concentration of H_2S measured from the treated gas sample was again 0.26 mg L^{-1}. One should note that this low value of H_2S concentration could be in fact a background reading and the actual value could be zero.

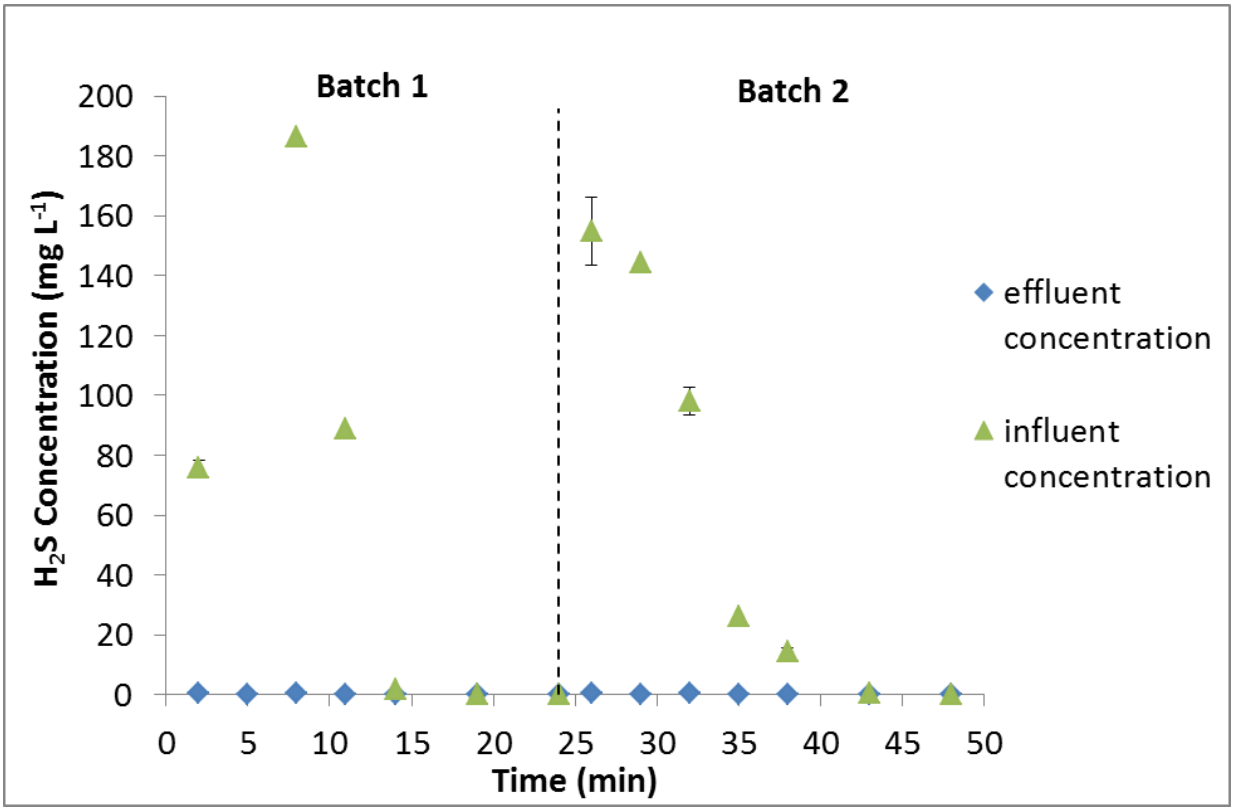

Figure 4.9. Reproducibility of semi-pilot scale test showing H_2S concentration profiles in the gases emitted from the swine manure (influent gas) and treated gas (effluent gas).

A control test was also performed in the semi-pilot scale test to verify if any component of the adsorption column has an effect on H_2S adsorption. As shown in Figure 4.10, there was no significant difference in the inlet and outlet concentrations. The highest standard deviation between the influent and effluent samples was 6.07 mg L^{-1}, which was observed 5 minutes after the start of the experiment.

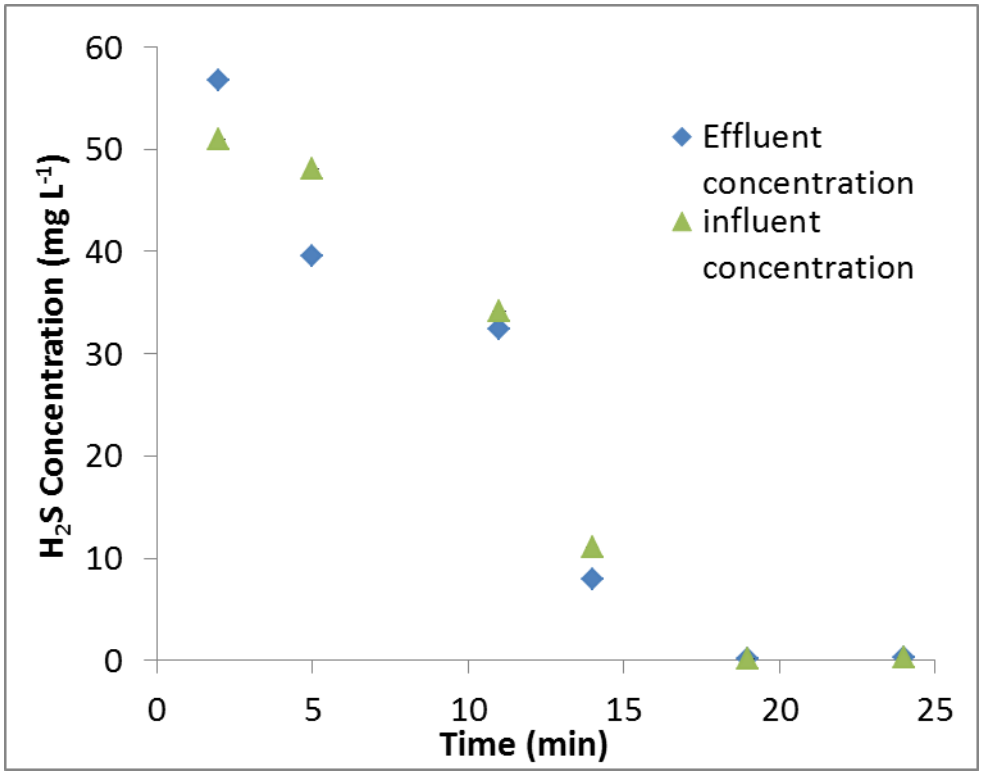

Figure 4.10. Control test showing H_2S concentration profiles in the gases emitted from the swine manure (influent gas) and treated gas (effluent gas).

The effectiveness of the ZnO nanoparticles in the capture of ammonia was also verified by analyzing the gas samples for ammonia concentration (Figure 4.11). The lowest and highest feed NH_3 concentration measured were 10 and 14 mg L^{-1}, respectively. The treated gas concentration measured ranged between 3-4 mg L^{-1}. This shows that ZnO nanoparticles were able to capture about 74% of ammonia that passed through the adsorption column. The reason for the lower adsorption efficiency compared to H_2S (almost 100% capture) is due to the type of the nanoparticles used. Zinc oxide nanoparticles are not very effective in capturing of ammonia and other type of nanoparticles (i.e. MgO) could be more effective. Alvarado et al. (2013) performed various tests using different nanoparticle types to assess their effectiveness in capturing H_2S and NH_3. They recorded that a relatively small amount of NH_3 was captured as compared to H_2S when ZnO nanoparticles were used. The reason was that there may be competition between H_2S and NH_3 molecules for the active sites on the ZnO nanoparticles (Alvarado et al., 2013).

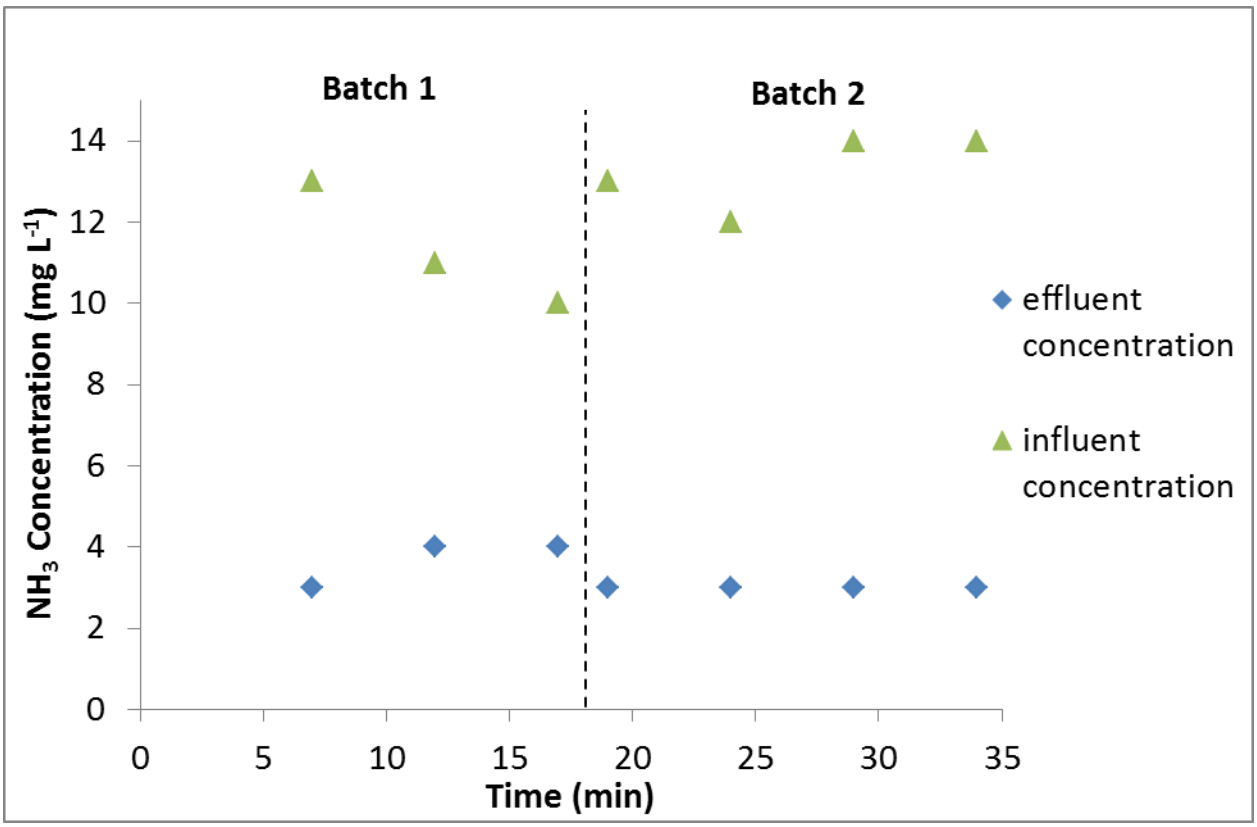

Figure 4.11. NH_3 concentration profiles in the gases emitted from the swine manure (influent gas) and treated gas (effluent gas).

The results from the laboratory scale tests provides information on the adsorption of H_2S on ZnO nanoparticles at different H_2S concentration, gas flow rate, nanoparticles size and quantity that may not be found in existing literature. Some of the results and trends observed in the breakthrough curves and capacities are also different from those in existing literature due to the differences in experimental conditions and adsorbent characteristics. This work was carried out with feed gas concentration ranging from 80 – 1700 mg L^{-1}, feed flow rate of 200 - mL min^{-1}, temperatures ranging from 1 – 41 °C using 18 or 80-20 nm nanoparticles.

5. CONCLUSIONS AND RECOMMENDATIONS FOR FUTURE WORK

5.1. Conclusions

Based on the results of the studies in the laboratory and semi-pilot tests, the following conclusions can be drawn:

1. The laboratory and semi-pilot tests proved that ZnO nanoparticles are effective in the removal of H_2S from contaminated gas stream at ambient temperatures. Although different nanoparticle sizes were used and experimental conditions were varied, the nanoparticles were able to take up H_2S in the contaminated air stream.

2. The equilibrium adsorption capacities increased and the ZnO nanoparticles reached saturation state faster with increased feed H_2S concentration. However, the breakthrough adsorption capacities were not drastically affected. Also, the effect of H_2S concentration on adsorption was more drastic at low concentration range (94.7 to 540.6 mg L^{-1}).

3. The use of larger ZnO nanoparticles caused the adsorbent to reach saturation state faster and to have lower adsorption capacities (both breakthrough and equilibrium capacities). This was observed for all the tested H_2S concentrations.

4. The increase in feed gas flow rate led to faster saturation rate but the breakthrough and equilibrium adsorption capacities were not impacted.

5. The results from the laboratory tests confirmed that the rate at which the adsorbent got saturated was not affected by increase of temperature (1, 11, 21 and 41 °C). There was also no significant effect on the breakthrough adsorption capacity. The equilibrium adsorption capacity, however, increased with an increase in temperature.

6. The results from the tests on the effects of adsorbent quantity showed that the adsorbent got saturated faster when the nanoparticles quantity was reduced regardless of the feed H_2S concentration. The breakthrough and equilibrium adsorption capacities also increased with increase in nanoparticle quantity.

7. Langmuir, Freundlich, Langmuir- Freundlich and BET isotherms were used to describe the laboratory experimental data. Among these, BET isotherm best described H_2S equilibrium data with the highest R^2 (coefficient of determination) among all evaluated isotherms.

8. The semi-pilot scale experiments clearly showed the effectiveness of ZnO nanoparticles in the capture of H_2S from a swine production facility (capturing efficiency higher than 99%).

9. The results from the semi-pilot scale tests showed that ZnO nanoparticles are not too effective in the capture of NH_3, with capturing efficiency being around 74%.

5.2. Recommendations for future work

1. A more extensive study on the effects of the various operating conditions in the semi-pilot scale setup in an actual production facility will assist in providing better information that is required for the design of an effective filtration system in an industrial facility. The results may be different from that of the laboratory tests because of the influence of other parameters such as composition of gas, humidity content, and temperature variations.

2. A detailed study on the removal of H_2S together with other hazardous gases such as NH_3 is recommended since industrial emissions comprise of several hazardous gases.

3. Preliminary studies have shown that ZnO nanoparticles are not too effective in removing NH_3 from contaminated airstream. Other nanoparticles (preferably MgO nanoparticles) should be used to test the removal of NH_3. It would be interesting to test the effectiveness of removal of NH_3 using the different experimental conditions (feed gas concentration, feed gas flow rate, temperature and adsorbent quantity) that were used in this thesis.

4. Application of this treatment technique at the barn scale is recommended to identify any unforeseen technical problems.

5. Chemical analysis of the nanoparticles should be conducted to provide information on changes in the chemical properties and structure of the nanoparticles before and after H_2S adsorption.

6. Research should be done into desorption and regeneration of the used nanoparticles. This will make the nanoparticles reusable and harmless to the environment.

7. A detailed analysis of the cost involved in application of nanoparticles to control hazardous gas emissions in swine production was not in the scope of the current study. However, to develop this technology for practical applications a thorough economic feasibility study following the completion of room scale evaluation will be required and recommended.

6. REFERENCES

ACGIH (American Conference of Governmental Industrial Hygienists). 2010. Hydrogen Sulfide: TLV Chemical Substances, 7th Edition. Publication #7DOC-316. Cincinnati, Ohio.

Ali, M. H. 2011. Ammonia gas adsorption on metal oxide nanoparticles. M.Sc. Thesis, Kansas State University. http://krex.k-state.edu/dspace/bitstream/handle/2097/13094/HasanMohammad2011.pdf?sequence=7 > Accessed: 1 August 2014.

Alvarado, A. C. 2011. Control of hydrogen sulfide, ammonia and odour emissions from swine barns using zinc oxide nanoparticles. M.Sc. Thesis. University of Saskatchewan, Saskatoon, Saskatchewan. Department of Chemical and Biological Engineering.

Alvarado A. C., B. Z. Predicala, D. A. Asis. 2013. Mixing nanoparticles with swine manure to reduce hydrogen sulfide and ammonia emissions. International Journal of Environmental Science Technology, 1-12.

An, S., K. Tang, M. Nemati. 2010. Simultaneous biodesulphurization and denitrification using an oil reservoir microbial culture: Effects of sulphide loading rate and sulphide to nitrate loading ratio. Water Research, 44, 1531-1541.

An, Y., K. Zhang, F. Wang, L. Lin, H. Guo. 2011. Removal of pollutants from water by nano-scale MgO particles: Feasibility and Disadvantage. Bioinformatics and Biomedical Engineering, (iCBBE) 2011 5th International Conference, 1-5.

Arogo, J., P. W. Westerman, A. J. Heber, W. P. Robarge, J. J. Classen. 2001. Ammonia emissions - A review. American Society of Agricultural and Biological Engineers paper No. 014089. St. Joseph, MI.

Arogo, J., R. H. Zhang, G. l. Riskowski, D. L. Day. 2000. Hydrogen sulfide production from store liquid swine manure: a laboratory study. Trans. American Society of Agricultural Engineers 43(5): 1241-1245.

Assaad, V., J. Jofriet, G. Hayward. 2008. Sulphate and sulphide corrosion in livestock buildings, Part I: Concrete deterioration. Biosystems Engineering 99, 372-381.

ASABE. 2005b. Manure storage safety. American Society of Agricultural and Biological Engineers standard EP470. St. Joseph, MI.

ASABE. 2007. Management of manure odours. American Society of Agricultural and Biological Engineers standard EP379.4. St. Joseph, MI.

Asis, D. A. 2008. Investigation of potential application of nanoparticles in reducing gas and odour emission from swine manure slurry. M.Sc. Thesis. University of Saskatchewan, Saskatoon, Saskatchewan. Department of Agricultural and Bioresource Engineering.

Atia, A., K. Haugen-Kozyra, M. Amrani. 2013. Ammonia and hydrogen sulfide emissions from livestock production. Manure Research Findings and Technologies: From Science to Social Issues [Online]. Alberta, Canada. <http://www1.agric.gov.ab.ca/$department/deptdocs.nsf/all/epw8313/$FILE/chapter7.pdf> Accessed: 1 August 2014.

ATSDR (Agency for Toxic Substances and Disease Registry). 2006. Public health statement: Hydrogen sulfide. CAS no. 7783-06-4. Division of Toxicology and Environmental Medicine, Atlanta, GA.

Bandosz, T. J., C. Petit. 2009. On the reactive adsorption of ammonia on activated carbons modified by impregnation with inorganic compounds. Journal of Colloids and Interface Science, 338, 330-344.

Banhazi, T. M., C. Saunders, N. Nieuwe, V. Lu, A. Banhazi. 2010. Oil spraying as an air quality improvement technique in livestock buildings: development and utilisation of a testing device. (technical paper). Australian Journal of Multi-disciplinary Engineering, 8(2), 169-177.

Barrasa, M., S. Lamosa, M. D. Fernandez, E. Fernandez. 2010. Occupational exposure to carbon dioxide, ammonia and hydrogen sulphide. Annals of Agricultural and Environmental Medicine, 19(1), 17-24.

Battye, R., W. Battye, C. Overcash, S. Fudge, 1994. Development and selection of ammonia emissions factors. EPA contract number 68-D3-0034, US Environmental Protection Agency.

Bicudo, J. R., C. J. Clanton, D. R. Schmidt, W. Powers, L. D. Jacobson, C. L. Tengman. 2004. Geotextile covers to reduce odour and gas emissions from swine manure storage ponds. Appld. Eng. in Agric., 20(1), 65-75.

Brunauer. S. 1943. The Adsorption of Gases and Vapors, vol. 1, Princeton University Press.

Bussink, D. W., O. Oenema, 1998. Ammonia volatilization from dairy farming systems in temperate areas: a review. Nutrient Cycling in Agroecosystems, 51, 20-30.

Cao, J., D. Elliott, W. -X. Zhang. 2005. Perchlorate reduction by nanoscale iron particles. Journal of Nanoparticle Research, 7, 499-506.

Casey, K. D., J. R. Bicudo, D. R. Schmidt, A. Singh, S. W. Gay, R. S. Gates, L. D. Jacobson, S. J. Hoff. 2006. Air quality and emissions from livestock and poultry production/ waste management systems. In Animal agriculture and the environment: National Center for Manure and Animal Waste Management White Papers, 1-40. J. M. Rice, D. F. Caldwell, F. J. Humenik (eds.). American Society for Agricultural and Biological Engineers St. Joseph, Michigan.

Chang, D. L., S. J. Lee, W. Y. Choi, K. S. Lee. 2004. A pilot scale biofilter system to reduce odour from swine operation. American Society of Agricultural Engineers Annual International Meeting. No. 044056. Ottawa, Ontario, Canada.

Chen, L., S. Hoff, L. Cai, J. Koziel. 2008. Odor reduction during biofiltration as affected by air flow rate and media moisture content. American Society of Agricultural and Biological Engineers meeting presentation paper no. 083859, pp. 3-16. Providence, Rhode Island.

CCOHS (Canadian Centre for Occupational Health and Safety), 2005. Cheminfo, <http://www.ccohs.ca/products/databeses/samples/cheminfo.html> Accessed: 1 August 2014.

Chenard, L., S. P. Lemay, C. Lague. 2003. Hydrogen sulphide assessment in shallow-pit swine housing and outside manure storage. Journal of Agricultural Safety and Health, 9(4), 285-302.

Chung, Y.-C., C. Huang, C. –P. Tseng, J. R. Pan, 1999. Biotreatment of H2S- and NH3-containing waste gases by immobilized cells biofilter. Chemosphere, 41(2000), 329-335.

Curtis, S. E. 1983. Environmental management in animal agriculture. Iowa: Iowa State University Press.

DeBruyn, J. 2000. Biofiltration for odour control from swine housing in Manitoba. M.Sc Thesis, University of Manitoba, Winnipeg, Manitoba. http://mspace.lib.umanitoba.ca/bitstream/1993/1879/1/MQ57529.pdf > Accessed: 1 August 2014.

Flood, E. A. (Ed). 1968. The solid-gas interface, vol. 1, no. 2, M. Dekker, New York.

Godbout, S., S. P. Lemay, R. Joncas, J. P. Larouche, D. Y. Martin, J. F. Bernier, R. Zijlstra, L. Chénard, A. Marquis, E. Barber, D. Massé. 2001. Oil sprinkling and dietary manipulation to reduce odour and gas emissions from swine buildings - Laboratory scale experiment. In Livestock Environment VI - Proceedings of the 6th International Symposium, 671-678. Louisville, Kentucky, USA: American Society of Agricultural Engineers, St. Joseph, MI.

Guo, J., Y. Luo, A. C. Lua, R. Chi, Y. Chen, X. Bao, S. Xiang. Adsorption of hydrogen sulphide (H_2S) by activated carbons derived from oil-palm shell. Carbon, 45(2), 30-336.

Haimour, N., R. El-Bishtawi, A. Ail-Wahbi, 2005. Equilibrium adsorption of hydrogen sulfide onto CuO and ZnO. Desalination, 181(1), 145-152.

Habibi, R., A. M. Rashidi, J. T. Daryan. 2010. Study of the rod-like and spherical nano-ZnO morphology on H_2S removal from natural gas. Applied Surface Science, 257(2), 434-439.

Hartung , J., T. Jungbluth, W. Buscher. 2001. Reduction of ammonia and odour emissions from a piggery with biofilters. Transactions of the American Society of Agricultural Engineers, 44, 113-118.

Hartung, E., V. R. Phillips, 1994. Control of gaseous emissions from livestock buildings and manure stores. Journal of Agricultural Engineering Research, 57, 173-189.

Heber, A. J.,T. T. Lim, P. C. Tao, J. Q. Ni. 2004. Control of air emissions from swine finishing buildings with recycled lagoon effluent. American Society of Agricultural Engineers Annual International Meeting, Paper no. 04-4156, 1-6. St Joseph, MI.

Hobbs, P. J., B. F. Pain, R. M. Kay, P. A. Lee. 1996. Reduction of odorous compounds in fresh pig slurry by dietary control of crude protein. Journal of the Science of Food and Agriculture, 71, 508-514.

Hu, J., G. Chen, I. Lo. 2005. Removal and recovery of Cr (VI) from wastewater by maghemite nanoparticles. Water Research, 39(18), 4528-4536.

Jacobson, L. D., D. R. Bicudo, D. R. Schmidt, S. Wood-Gay, R. S. Gates, S. J. Hoff. 2003. Air emissions from animal production buildings. In Proceedings XI International Congress International Society for Animal Hygyiene (ISAH), 119-135. Tartu, Estonia: ISAH.

Jain, P., T. Pradeep. 2005. Potential of silver nanoparticle-coated polyurethane foam as an antibacterial water filter. Biotechnology and bioengineering, 90(1), 59-62.

Jongbloed, W., N. P. Lenis. 1992. Alteration of nutrients as a means to reduce environmental pollution by pigs. Livestock Production Science, 31, 75-90.

Ju-Nam, Y., J. R. Lead, 2008. Manufactured nanoparticles: An overview of their chemistry, interactions and potential environmental implications. Science of the Total Environment, 400, 396-407.

Kendall, D. C., K. M. Lemenager, B. T. Richert, A. L. Sutton, J. W. Frank, B. A. Belstra, D. Bundy. 1998. Effects of intact protein diets versus reduced crude protein diets supplemented with synthetic amino acids on pig performance and ammonia levels in swine buildings. Swine Day, 141-146.

Khaleel, A., P. N. Kapoor, K. J. Klabunde. 1999. Nanocrystalline metal oxides as new adsorbents for air purification. Pergamon, 11(4), 459-467.

Khalfaoui, M. S. Knani, M. A. Hachicha, A. Ben Lamine. 2003. New theoretical expressions for the five adsorption type isotherms classified by BET based on statistical physics treatment. Journal of Colloid and Interface Science, 263, 350-356.

Kim, Y.-K., H. J. Ko, H. T. Kim, Y. S. Kim, Y. M. Roh, C. M. Lee, C. N. Kim. 2008. Odor reduction rate in the confinement pig building by spraying various additives. Bioresource Technology, 99(17), 8464-8469.

Koppolu, L., R. Koelsch, D. Schulte, C. Powers, D. Bundy. 2005. A new application for fine ground rubber in the control of odours from livestock manure storage structures. American Society of Agricultural and Biological Engineers Paper no. 054052, 1-10. Tampa, FL.

Kurvits, T., T. Marta. 1998. Agricultural NH_3 and NOx emissions in Canada. Environmental Pollution, 102(S1), 187-189.

Le, P. D., A. J. Aarnink, A. W. Jongbloed 2009. Odour and ammonia emission from pig manure as affected by dietary crude protein level. Livestock Science, 121, 267-274.

Lee, Y. J., N. –K. Park, G. B. Han, S. O. Gyu, T. J. Lee, C. H. Chang. 2007. The preparation and desulfurization of nano-size ZnO by a matrix-assisted method for the removal of low concentration of sulfur compounds. Current Applied Physics 8, 746-751.

Lemay, S. 1999. Barn management and control of odours. Advances in Pork Production, 10, 81.

Martens, W., M. Milos, R. Zapiran, S. Marcus, E. Hartung, U. Palmgren. 2000. Reduction potential of microbial, odour and ammonia emissions from a pig facility by biofilters. International Journal of Hygiene and Environmental Health, 336-344.

Masciangioli, T., W. –X. Zhang. 2003. Environmental technologies at the nanoscale. Environmental Science and Technology, 37(5), 102-106.

McCrory, D. F., P. J. Hobbs. 2001. Additives to reduce ammonia and odor emissions from livestock wastes: A review. Journal Environmental Quality, 30, 345-355.

McGinn, S. M., K. M. Koenig, T. Coates. 2002. Effect of diet on odorant emissions from cattle manure. Canadian Journal of Animal Science, 82, 435-442.

Moreno, L., B. Predicala, M. Nemati. 2010. Laboratory, semi-pilot and room scale study of nitrite and molybdate mediated control of H_2S emission from swine manure. Bioresource Technology, 101, 2141-2151.

Morris, J., J. Willis, K. Gallagher. 2007. Nanotechnology white paper. US Environmental Protection Agency, 4-10.

Nassar, N. P. Pereira-Almao. 2010. Capturing $H_2S_{(g)}$ by in situ-prepared ultradispersed metal oxide particles in an oilsand-packed bed column. Energy Fuels, 24(11), 5903-5906.

Nicolai, R. E., K. A. Janni. 1997. Development of a low cost biofilter for swine production facilities. American Society of Agricultural Engineers meeting Paper No. 974040, 1-7. St. Joseph, MI.

Nicolai, R. E., K. A. Janni. 2001. Determining pressure drop through compost-wood chip biofilter media. American Society of Agricultural Engineers annual International meeting Paper no. 014080. Sacramento, California.

Nicolai, R. E., C. J. Clanton, K. A. Janni, G. L. Malzer. 2006. Ammonia removal during biofiltration as affected by inlet air temperature and media moisture content. Transactions of the American Society of Agricultural and Biological Engineers, 49(4), 1125-1138.

Niemeyer, C. M. 2001. Nanoparticles, proteins, and nucleic acids: Biotechnology Meets Materials Science. Angewandte Chemie International Edition, 40(22).

NIOSH. 2007. Pocket guide to chemical hazards. NIOSH Publication no. 2005-149. Washington D.C. National Institute for Occupational Safety and Health. http://www.cdc.gov/niosh/docs/2005-149/pdfs/2005-149.pdf > Accessed: 1 Aug 2013.

Novochinskii, I. I., C. Song, X. Ma, X. Liu, L. Shore, J. Lampert, R. J. Farrauto. 2004. Low-temperature H_2S removal from steam-containing gas mixtures with ZnO for fuel cell application. 1. ZnO particles and extrudates. Energy & fuels, 18(2), 576-583.

Okuyama, K., M. Abdullah, W. Lenggoro, F. Iskandar 2006. Preparation of functional nanostructured particles by spray drying. Advanced Powder Technology, 17(6), 587-610.

Olivier, J. G., A. F. Bouwman, K. W. Van der Hoek, J. J. Berdowski. 1998. Global air emission inventories for anthropogenic sources of NOx, NH_3 and N_2O in 1990. Environmental Pollution, 102(S1), 135-148.

Olivera, R., P. Mauricio, G. Jr. Oswaldo. 2011. Biosorption of Metals: State of the Art, General Features, and Potential Applications for Environmental and Technological Processes, Progress in Biomass and Bioenergy Production, Dr. Shahid Shaukat (Ed.), ISBN: 978-953-307-491-7,

InTech, DOI: 10.5772/17802. Available from: <http://www.intechopen.com/books/progress-in-biomass-and-bioenergy-production/biosorption-of-metals-state-of-the-art-general-features-and-potential-applications-for-environmental> Accessed: 1 August 2014.

OSHA. 2001. Hydrogen Sulfide: OSHA Chemical Sampling Information. Washington, D.C., Occupational Safety and Health Administration. http://www.osha.gov/dts/chemicalsampling/data/CH_246800.html > Accessed: 1 August 2014.

Osorio, J. A., I. F. Tinoco, H. J. Ciro. 2009. Ammonia: A review of concentration and emission models in livestock structures. Dyna, 76(159), 89-99.

Ouellette, C., S. Lemay, S. Godbout, I. Edeogu. 2006. Oil application to reduce dust and odour emissions from swine buildings ouellette. CSBE/SCGAB 2006 Annual Conference. No. 06-147. Edmonton, Alberta.

Park, K. J., J. Zhu, Z. Zhang. 2005. Influence of aeration rate and liquid temperature on ammonia emission rate and manure degradation in batch aerobic treatment. Transactions-American Society of Agricultural Engineers, 48(1), 321-330.

Portejoie, S., J. Martinez, F. Guiziou, C. M. Coste. 2003. Effect of covering pig slurry stores on the ammonia emission process. Bioresource Technology, 87, 199-207.

Powers, W. 2004. Practices to reduce hydrogen sulfide from livestock operations. Environmental Quality 4(1). Iowa State University Extention Publication.

Predicala, B., M. Nemati, S. Stade, C. Lague. 2008. Control of H_2S emission from swine manure using Na-nitrite and Na-molybdate. Journal of Hazardous Materials, 154, 300-309.

Riskowski, G. L. 2004. Overview of methods to reduce odorant omissions from confinement swine buildings, swine odours and waste management. University of Illinois. <http://www.livestocktrail.illinois.edu/uploads/sowm/papers/p122-128.pdf > Accessed: 1 August 2014.

Rosso, I., C. Galletti, M. Bizzi, G. Saracco, V. Specchia. 2003. Zinc oxide sorbents for the removal of hydrogen sulfide from syngas. Industrial & Engineering Chemistry Research, 42(8), 1688-1697.

Rouquerol, J., F. Rouquerol, K. S. Sing. 1999. Absorption powders and porous solids. Academic press.

Sayyadnejad, M. A., H. R. Ghaffarian, M. Saeidi. 2008. Removal of hydrogen sulfide by zinc oxide nanoparticles in drilling fluid. International Journal for Science and Technology, 5(4), 565-569.

Schneegurt, M. A., D. L. Weber, S. Ewing, H. B. Schur. 2005. Evaluating biostimulant effects in swine production facility wastewater. In Proceedings of State of the Science of Animal Manure and Waste Management Symposium. 1-6. San Antonio, Texas: National Center for Manure and Animal Waste Management.

Schmidt, A. M., A. J. Heber. 2004. Dust, gas and odour control in swine finishing barns through oil sprinkling. Swine Management, Agricultural MU guide. MU Extention, University of Missouri-Columbia.

Shah, S., P. Westerman, G. Grabow. 2007. Additives for improving hog farm air quality. North Carolina Cooperation Extention Service, North Carolina State University. https://www.bae.ncsu.edu/programs/extension/publicat/wqwm/AG-686w.pdf > Accessed: 1 August 2014.

Simo, M., S. Sivashanmugam, C. J. Brown, V. Hlavacek. 2009. Adsorption/desorption of water and ethanol on 3A zeolite in near-adiabatic fixed bed. Industrial & Engineering Chemistry Research, 48(20), 9247-9260.

Sing, K. S. W., D. H. Everett, R. A. W. Haul, L. Moscou, R. A. Pierotti, J. Rouque´rol, T. Siemieniewska. 1985. Reporting physisorption data for gas/solid systems with special reference to the determination of surface area and porosity. Pure and Applied Chemistry, 57, 603–619.

Song, H. S., M. G. Park, S. J. Kwon, K. B. Yi, E. Croiset, Z. Chen, S. C. Nam. 2013. Hydrogen sulfide adsorption on nano-sized zinc oxide/reduced graphite oxide composite at ambient condition. Applied Surface Science, 276, 646-652.

Smith, D. R., P. A. Moore, J. B. Haggard, C. V. Maxwell, T. C. Daniel, K. VanDevander, M. E. Davis. 2004. Effect of aluminium chloride and dietary phytase on relative ammonia losses from swine manure. Journal of Animal Science, 82, 605-611.

Statistics Canada. 2012. Hog statistics. Catalogue no. 23-010-X. Second quarter. < http://www.statcan.gc.ca/pub/23-010-x/23-010-x2012003-eng.pdf> Accessed: 6 August 2014>

Statistics Canada. 2014. Livestock estimates. Catalogue no. 11-001-X. < http://www.statcan.gc.ca/daily-quotidien/140305/dq140305a-eng.pdf> Accessed: 6 August 2014

Sun, J., S. Modi, K. Liu, R. Lesieur, J. Buglass. 2007. Kinetics of zinc oxide sulfidation for packed-bed desulfurizer modeling. Energy & fuels, 21, 1863-1871.

Sutton, A. L., K. B. Kephart, M. W. Verstegen, T. T. Canh, P. J. Hobbs. 1999. Potential for reduction of odorous compounds in swine manure through diet modification. Journal of Animal Science, 77, 430-439.

Sutton, A., T. Applegate, S. Hankins, B. Hill, D. Sholly, G. Allee, W. Greene, R. Kohn, D. Meyer, W. Powers, T. vanKempen. 2001. Manipulation of animal diets to affect manure production, composition and odors: State of the science. In Animal Agiculture and the Environment, National Center for Manure and Animal Waster Management White Papers, Rice, J. M,, D. F. Caldwell, F. J. Humenik, (Eds.) American Society for Agricultural Engineers publication no. 913C0306. St. Joseph, MI. 377-408. 1-3.

Svard, T. 2004. Adsorption of hydrogen sulfide at low temperature. Lund University, Lund, Sweden. http://www.chemeng.lth.se/exjobb/E093.pdf > Accessed: 20 March 2013.

Tiede, K., M. Hassellov, E. Breitbarth, Q. Chaudhry, A. B. Boxall, 2009. Considerations for environmental fate and ecotoxicity testing to support environmental risk assessments for engineered nanoparticles. Journal of Chromatography A, 1216, 503-509.

Veeman, T. S., R. Gray. 2009. Agricultural production and productivity in Canada. Choices, 24(4).

Wang, X., T. Sun, J. Yang, L. Zhao, J. Jia. 2008. Low-temperature H_2S removal from gas streams with SBA-15 supported ZnO nanoparticles. Chemical Engineering Journal, 142(1), 48-55.

Xiao, Y., S. Wang, D. Wu, Q. Yuan. 2008. Experimental and simulation study of hydrogen sulfide adsorption on impregnated activated carbon under anaerobic conditions. Journal of hazardous materials, 153(3), 1193-1200.

Zhang, S. 2011. Air quality and community health impact of animal management. National Collaborating Centre for Environmental Health.

7. APPENDICES

A. Supplementary experimental data

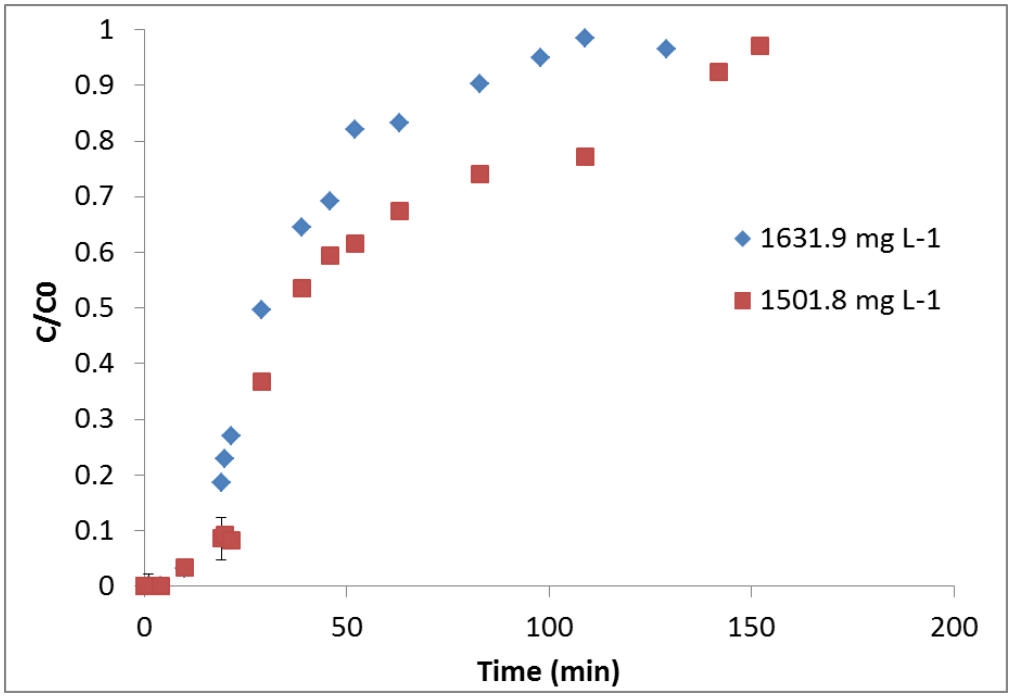

Figure A.1. Reproducibility of breakthrough curves for H_2S adsorption on ZnO nanoparticles (18 nm) for feed H_2S concentration of 1501.8 and 1631.9 mg L^{-1} at 21 °C.

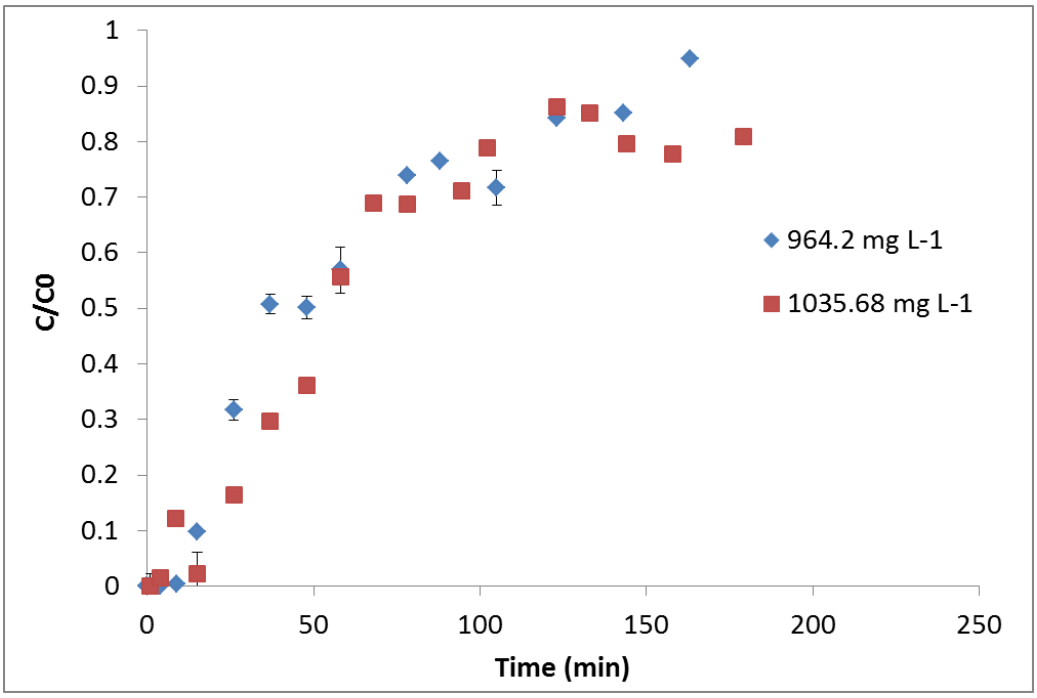

Figure A.2. Reproducibility of breakthrough curves for H_2S adsorption on ZnO nanoparticles (18 nm) for feed H_2S concentration of 964.2 and 1035.68 mg L^{-1} at 21 °C.

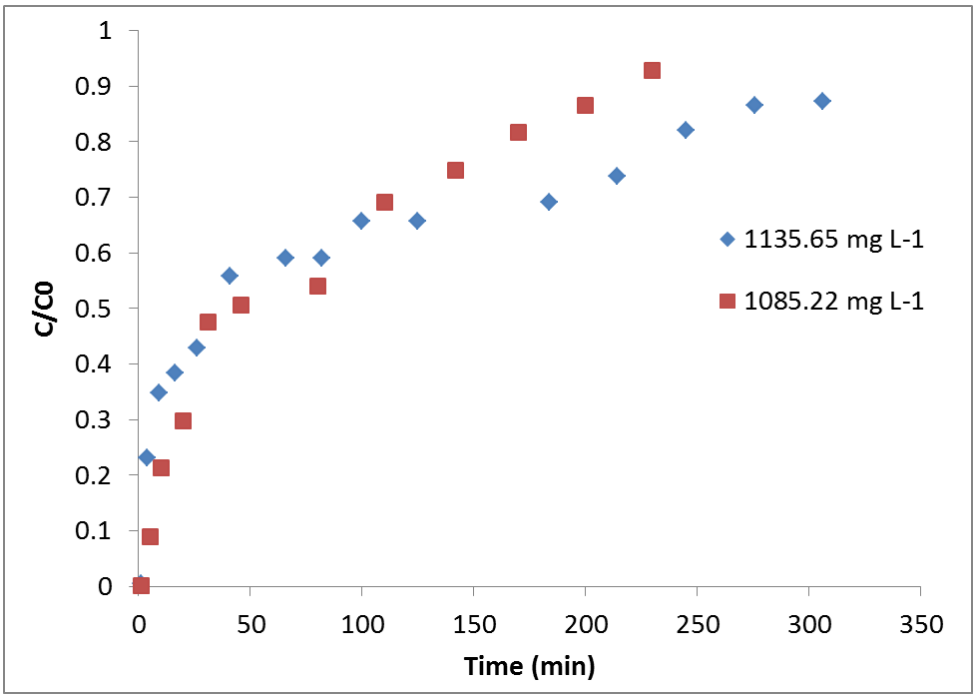

Figure A.3. Reproducibility of breakthrough curves for H_2S adsorption on ZnO nanoparticles (18 nm) for feed H_2S concentration of 1135.65 and 1085.22 mg L^{-1} at 41 °C.

B. Gas chromatograph calibration curves for H_2S

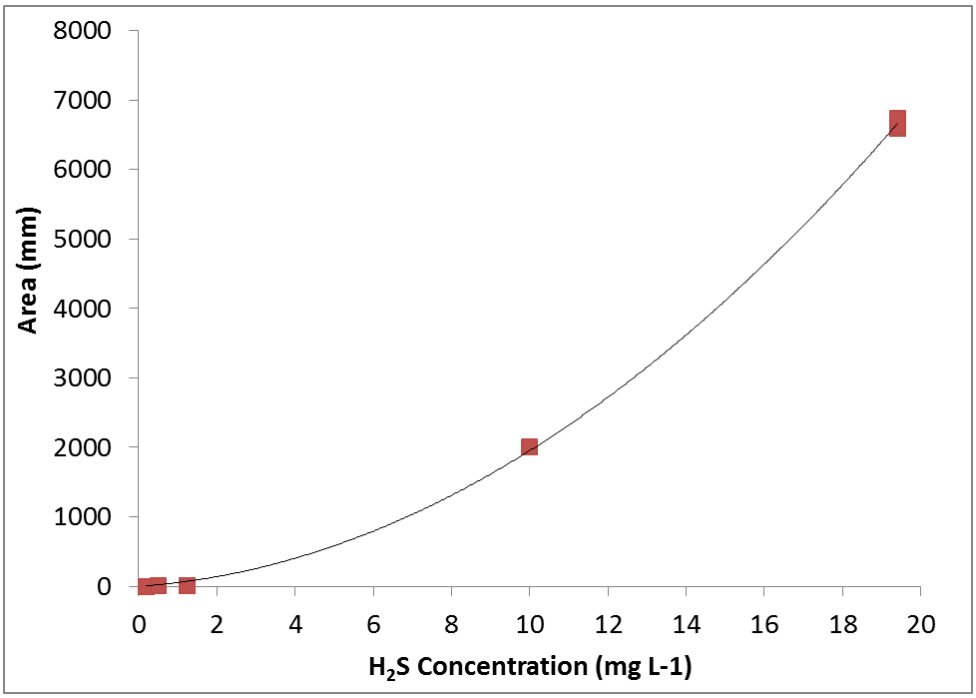

Figure B.1. Gas Chromatograph calibration curve for 0 to 19.4 mg L^{-1} range.

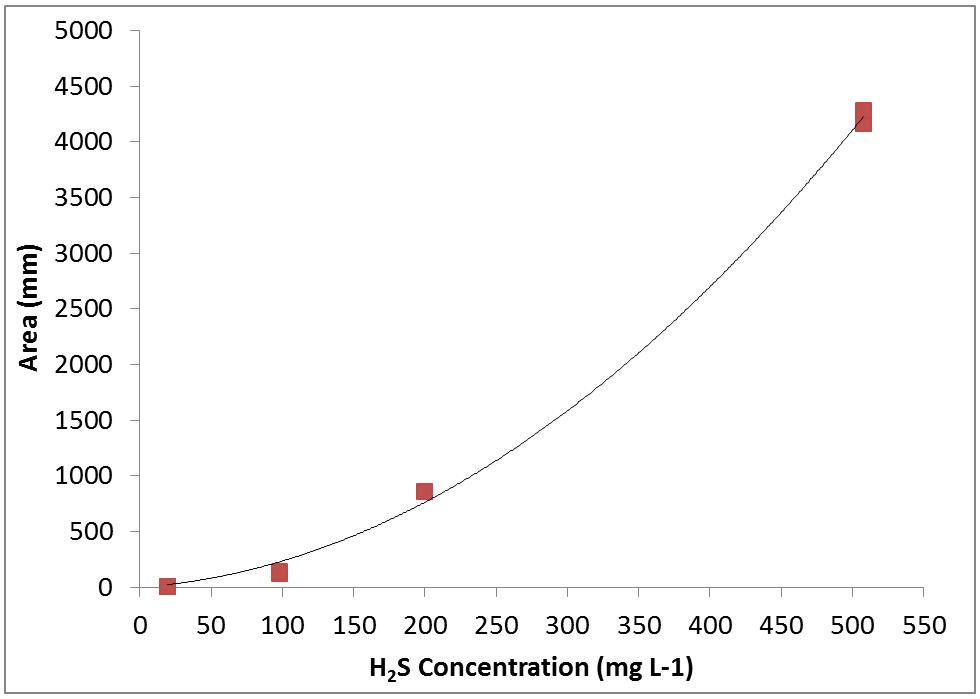

Figure B.2. Gas Chromatograph calibration curve for 19.4 to 508 mg L^{-1} range.

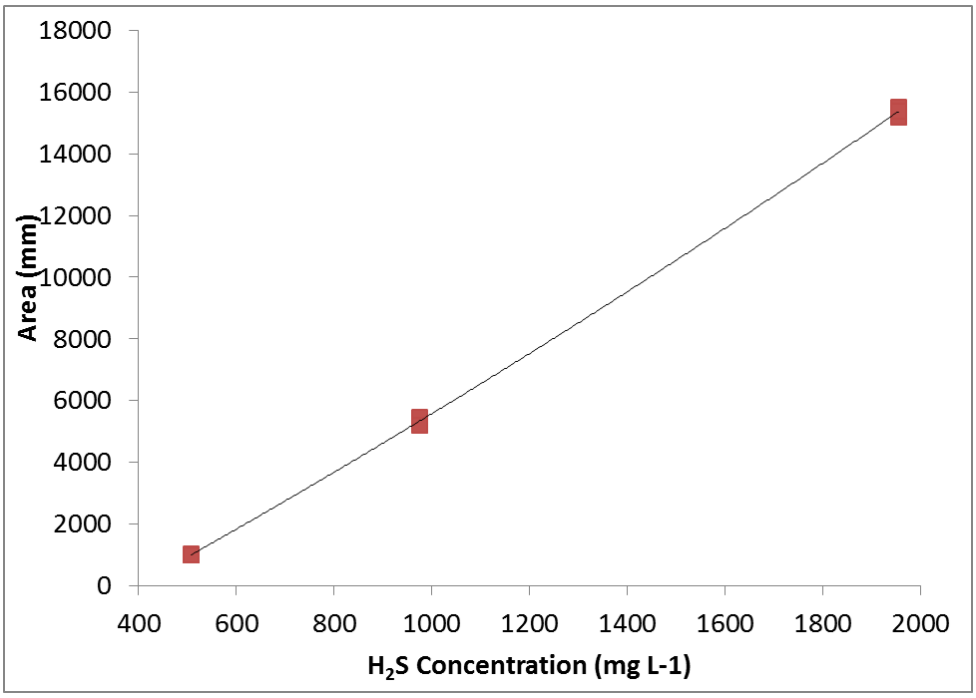

Figure B.3. Gas Chromatograph calibration curve for 508 to 2000 mg L^{-1} range.

C. Surface area, pore volume and pore size of nanoparticles

Table C.1. Surface area of nanoparticles

Surface Area	Fresh 18 nm ZnO nanoparticles	Fresh 80-200 nm ZnO nanoparticles
Single point surface area at p/p° = 0.300083521	26.1764 m^2/g	10.9572 m^2/g
BET Surface Area	26.4785 m^2/g	11.3659 m^2/g
Langmuir Surface Area	36.3919 m^2/g	15.7359 m^2/g
t-Plot Micropore Area	5.4574 m^2/g	-
t-Plot External Surface Area	21.0212 m^2/g	12.2246 m^2/g
BJH Adsorption cumulative surface area of pores between 1.7000 nm and 300.0000 nm width	24.666 m^2/g	11.112 m^2/g
BJH Desorption cumulative surface area of pores between 1.7000 nm and 300.0000 nm width	26.2644 m^2/g	11.5525 m^2/g

Table C.2. Pore volume of nanoparticles

Pore Volume	18 nm ZnO nanoparticles	80-200 nm ZnO nanoparticles
Single point adsorption total pore volume of pores less than 127.5252 nm width at p/p° = 0.984584047	0.116184 cm^3/g	0.022675 cm^3/g
Single point desorption total pore volume of pores less than 92.8033 nm width at p/p° = 0.978684113	0.133791 cm^3/g	0.019916 cm^3/g
t-Plot Micropore volume	0.002490 cm^3/g	-0.000638 cm^3/g
BJH Adsorption cumulative volume of pores between 1.7000 nm and 300.0000 nm width	0.146811 cm^3/g	0.026646 cm^3/g
BJH Desorption cumulative volume of pores between 1.7000 nm and 300.0000 nm width	0.147897 cm^3/g	0.026027 cm^3/g

Table C.3. Pore Size of nanoparticles

Pore Size	**18 nm ZnO nanoparticles**	**80-200 nm ZnO nanoparticles**
Adsorption average pore width (4V/A by BET)	17.55147 nm	7.97983 nm
Desorption average pore width (4V/A by BET)	20.21128 nm	7.00899 nm
BJH Adsorption average pore width (4V/A)	23.8080 nm	9.5922 nm
BJH Desorption average pore width (4V/A)	22.5243 nm	9.0118 nm